LABORATORY INVESTIGATION OF LOW-DENSITY PLASMAS BY CONTINUOUS-WAVE LASER SCATTERING

by

Harry Coleman Koons

S.B., Massachusetts Institute of Technology

(1963)

SUBMITTED IN PARTIAL FULFILLMENT

OF THE REQUIREMENTS FOR THE

DEGREE OF DOCTOR OF

PHILOSOPHY

at the

MASSACHUSETTS INSTITUTE OF

TECHNOLOGY

February, 1968

Signature of Author.....
Department of Geology and Geophysics, February 5, 1968

Certified by.....
Thesis Supervisor

Accepted by.....
Chairman, Departmental Committee
on Graduate Students

LABORATORY INVESTIGATION OF LOW-DENSITY PLASMAS BY CONTINUOUS-WAVE LASER SCATTERING

by

Harry Coleman Koons

Submitted to the Department of Geology and Geophysics
on February 5, 1968, in partial fulfillment of
the requirements for the degree of
Doctor of Philosophy.

ABSTRACT

The electron density and temperature in a low-density reflex discharge in helium have been measured by observing the radiation scattered from the beam of a continuous-wave argon ion laser. A synchronous detection system was used to distinguish the scattered radiation from all other radiation entering the detector.

The principal experimental results of this work are the successful use of cw laser scattering for plasma diagnostics, and the observation of an asymmetry in the electron temperature in the discharge. The electron temperature parallel to an imposed magnetic field was found to be 30,800 ^{o}K. The temperature perpendicular to the field was found to be 13,750 ^{o}K. This latter value agreed reasonably well with the value obtained from a plane Langmuir probe whose face was parallel to the magnetic field lines. The temperature asymmetry is qualitatively explained in terms of the energy sources and the velocity randomizing processes in the discharge.

The scattering measurements indicated an electron density of 4.8×10^{18} m^{-3}. This value is in good agreement with the value obtained with a Langmuir probe.

Thesis Supervisor: Giorgio Fiocco

Title: Assistant Professor of Geophysics

ACKNOWLEDGEMENTS

During the period of the author's thesis research, many persons contributed toward overcoming the problems associated with such an undertaking. Principal thanks go to his thesis supervisor, Professor Giorgio Fiocco, for providing the climate in which the work could be carried out, as well as for many discussions concerning details of the research itself.

The author is also thankful for valuable discussions and advice from Professor George Bekefi.

The author is indebted to Jacques B. Thompson, Al Ferragamo, and David Kitrosser for technical and other aid to this project. He would also like to thank his wife, Ann, for her help, patience, and moral support.

The use of the facilities of the Research Laboratory of Electronics and of the Francis Bitter National Magnet Laboratory is gratefully acknowledged.

This work was supported in part by the U.S. Army, the Air Force Office of Scientific Research, and the Office of Naval Research, and in part by the National Aeronautics and Space Administration under Grant NGR 22-009-131.

TABLE OF CONTENTS

LIST OF FIGURES

LIST OF TABLES

CHAPTER I

INTRODUCTION

The temperature and density of electrons in a plasma can be obtained from the spectrum and intensity of electromagnetic radiation scattered from the plasma [Gordon, 1958; Fejer, 1960a; Dougherty and Farley, 1960a; Salpeter, 1960a]. The detection of electromagnetic radiation scattered from a plasma was first accomplished by Bowles in 1958. He used a high-power pulsed radar operating at 41 MHz to obtain backscatter from the electrons in the ionosphere. Early observations of the scattering of laser radiation by electrons in an electron beam and in a laboratory plasma have been reported by Fiocco and Thompson [1963a] and Thompson and Fiocco [1963a]. In these, as well as in several other experiments carried out by different investigators, pulsed ruby lasers were used as the radiation sources. Preliminary work on the detection of Thomson scattering with a cw laser has been reported by Farrow and Buchsbaum [1965].

A. Brief Description of the Experiment

In plasma scattering experiments, the spectrum of the scattered radiation is characterized by the parameter $\alpha = \lambda_o/4\pi D\sin\frac{\theta}{2}$, where λ_o and D are the wavelength of the incident radiation and the Debye length respectively, and θ is the scattering angle. For $\alpha << 1$, the shape of the spectrum is Gaussian with a width determined by the electrom temperature. This thesis describes an experiment designed to operate in this regime. The electron temperature in a reflex discharge was measured both parallel and perpendicular to an imposed magnetic field by observing the radiation scattered from

the beam of a continuous-wave argon ion laser.

Both the plasma current and the laser light were modulated to permit synchronous detection of the scattered radiation and rejection of the background. The scattered radiation was observed at a scattering angle of approximately 8^{o} in two planes, one parallel and the other perpendicular to the magnetic field. The spectrum of the scattered radiation was obtained by rotating a narrow-band interference filter. The electron temperature and density obtained from the scattering data are compared to those obtained from Langmuir probe data.

B. Scope of this Thesis

Chapter II contains a review of the electromagnetic scattering theory pertinent to plasma scattering experiments. Scattering from a single charged particle is discussed first. This is followed by the scattering theory for thermal and nonthermal plasmas. Finally, the effect of an imposed magnetic field is discussed.

Chapter III contains a summary of earlier scattering experiments. In Chapter IV the cw laser is compared with the pulsed ruby laser as a radiation source for plasma scattering experiments. Chapter V describes the experimental apparatus used for the scattering measurements. The experimental results are presented in Chapters VI and VII and are discussed in Chapter VIII.

CHAPTER II

SCATTERING OF ELECTROMAGNETIC RADIATION BY CHARGED PARTICLES

Recent interest in the information which may be obtained by observing the electromagnetic radiation scattered by charged particles dates from a suggestion by Gordon [1958] that the incoherent scattering of radio waves by free electrons might be a powerful means of measuring the electron density and electron temperature as a function of height and time in the earth's ionosphere. Using the theory for Thomson scattering by independent charged particles, Gordon predicted that a broadening of the spectrum of the scattered radiation would result from the Doppler shifts caused by the thermal motion of the electrons. He estimated that the spread in frequencies in backscatter from the ionosphere would be of the order of 100 kHz at an operating frequency of 200 MHz. This technique has since been used to measure these parameters above the peak of the electron density in the F2 region. This region is not accessible unless the incident frequency is higher than the plasma frequency corresponding to the peak electron density. Thus, the region above the F2 peak cannot be reached by conventional ionosounding from the surface of the earth.

The first experiment [Bowles, 1958] obtained a much narrower spectral width than that predicted by Gordon. The information that has been obtained from such ionospheric backscatter experiments is reviewed in Chapter III. These experiments led to a number of papers which presented theoretical calculations of the scattered spectrum for monochromatic incident radiation scattered from a thermal, unmagnetized plasma. These calculations are

summarized in Section II-B. Later papers, which developed the theory for nonequilibrium plasmas, and for plasmas in a magnetic field, are reviewed in Section II-C.

The high electric field intensities available from a laser source may make possible a number of nonlinear plasma scattering effects which have been discussed in the literature. These include: relativistic effects; light-off-light scattering experiments with the plasma as the active medium, such as harmonic generation and beat generation; and scattering from driven plasma oscillations. These topics are briefly reviewed in Section II-E.

With the advent of the laser, scattering experiments could be performed at optical and infrared wavelengths using laboratory plasmas. Experiments using pulsed ruby lasers are reviewed in Chapter III.

A. Thomson Scattering of Radiation

Electromagnetic scattering by an isolated free charged particle is known as Thomson scattering. The following discussion follows the presentation by Jackson [1962]. If a plane wave of monochromatic radiation is incident on an isolated free particle of charge e and mass m, the particle is accelerated and thus emits radiation. This radiation is emitted in all directions, and the wavelength is Doppler shifted by the velocity of the particle with respect to the observer.

The instantaneous power radiated per unit solid angle by the accelerated particle is given by

$$\frac{dP}{d\Omega} = \frac{e^2}{16\pi^2 \varepsilon_o c^3} \left(\frac{d\vec{v}}{dt}\right)^2 \sin^2 \psi, \qquad (2.1)$$

where ψ is the angle between the direction of observation and the acceleration vector, which is along the electric vector of the incident wave. If the propagation vector of the incident radiation is $\vec{K}_o$, its electric field may be written as

$$\vec{E}(\vec{r},t) = \vec{E}_o \exp[i(\omega_o t - \vec{K}_o \cdot \vec{r})]. \tag{2.2}$$

From the force equation, we find that the particle's acceleration is

$$\frac{d\vec{v}}{dt} = \frac{e}{m} \vec{E}_o \exp[i(\omega_o t - \vec{K}_o \cdot \vec{r})]. \tag{2.3}$$

Then the average power radiated per unit solid angle can be written

$$\left\langle \frac{dP}{d\Omega} \right\rangle = c\varepsilon_o |E_o|^2 \left(\frac{e^2}{4\pi\varepsilon_o mc^2} \right)^2 \sin^2\psi. \tag{2.4}$$

The quantity $\frac{e^2}{4\pi\varepsilon_o mc^2} = r_e$ is known as the classical radius of the electron and has the magnitude 2.818×10^{-15} meters.

It is convenient to introduce a differential scattering cross section defined by

$$\frac{d\sigma}{d\Omega} = \frac{\text{Energy radiated/unit time/unit solid angle}}{\text{Incident energy flux/unit area/unit time}}. \tag{2.5}$$

The incident energy flux is the time-averaged Poynting's vector for the plane wave, namely, $I_o = \sqrt{\frac{\varepsilon_o}{\mu_o}} |E_o|^2$. Thus, from Eqs. 2.4 and 2.5 we may write the differential scattering cross section as

$$\frac{d\sigma}{d\Omega} = r_e^2 \sin^2\psi = 7.95 \times 10^{-30} \sin^2\psi. \tag{2.6}$$

The total scattering cross section, called the Thomson cross section, is

$$\sigma_t = \frac{8\pi}{3} r_e^2 = 6.65 \times 10^{-29} \text{ m}^2. \tag{2.7}$$

If the radiation is scattered by a moving particle, the frequency is Doppler shifted by an amount

$$\frac{\Delta f}{f} = \frac{\Delta \omega}{\omega} = \frac{2v}{c} \sin \frac{\theta}{2} , \tag{2.8}$$

where v is the velocity of the particle, and θ is the angle between the incident and the scattered wave vectors. This gives rise to a spectrum of scattered frequencies if the scattering is from an assembly of moving particles.

If their velocity distribution is $F(\vec{v})$, where $F(\vec{v})$ is normalized so that $\int_{-\infty}^{+\infty} F(\vec{v}) d\vec{v} = 1$, and if each electron may be assumed to scatter independently, then the average power scattered per unit solid angle per unit frequency interval is

$$\left\langle \frac{dP}{d\Omega d\omega} \right\rangle = \frac{d\sigma}{d\Omega} I_o N_e F(\vec{v}) = \frac{d\sigma}{d\Omega} I_o N_e F\left(\frac{\omega - \omega_o}{\kappa_o} \right), \tag{2.9}$$

where $\kappa_o = 2 K_o \sin \frac{\theta}{2}$.

In the special case that the velocity distribution is Maxwellian, this equation becomes:

$$\left\langle \frac{dP}{d\Omega d\omega} \right\rangle = \frac{\frac{d\sigma}{d\Omega} I_o N_e}{\kappa_o} \left(\frac{m}{2\pi k T_e} \right)^{1/2} \exp\left\{ - \frac{m}{2k T_e} \left(\frac{\omega - \omega_o}{\kappa_o} \right)^2 \right\} . \tag{2.10}$$

Then the spectrum of the scattered radiation is a Gaussian with a full width at half-height (FWHH) equal to

$$\Delta \omega = 2\kappa_o [(2k T_e/m) \ln 2]^{1/2} . \tag{2.11}$$

Eq. 2.11 may be used to determine the temperature of the electrons from the spectrum of the scattered radiation.

The ratio of the cross section for ions to the cross section for

electrons is

$$\frac{\sigma_+}{\sigma_-} = \left(\frac{Z^2 m}{M}\right)^2 . \qquad (2.12)$$

Thus the contribution from the ions is negligible in scattering experiments. This does not imply that scattering cannot be used to measure the properties of the ions. They are, in fact, put in evidence through their collective effects on the electron density fluctuations on a scale larger than the Debye length.

B. Scattering from a Thermal, Unmagnetized Plasma

Several authors have reported theoretical calculations of the intensity and spectrum of monochromatic, plane wave radiation scattered from an unmagnetized, equilibrium plasma [Salpeter, 1960a,b; Fejer, 1960a,b; Dougherty and Farley, 1960; Feix, 1965]. Computed profiles of the spectrum have been presented by Gerry and Patrick [1965] and Williamson et al. [1966].

The Magneto-ionic theory replaces the electrons by a continuous medium, whose index of refraction varies slowly in space and time. In a plasma there are, however, thermally driven fluctuations in the electron density. These produce fluctuations in the index of refraction which leads to scattering.

Consider a plane monochromatic wave of radian frequency ω_o and wave vector $\vec{K}_o$ incident on a volume V imbedded in a plasma. The scattered wave is assumed to have the same wave number with a wave vector $\vec{K}_s$ making an angle θ with respect to the incident wave vector. The plasma has a mean dielectric constant ε, and the thermal electron density fluctuations cause deviations $\delta\varepsilon(\vec{r},t)$ from this mean. At a very large distance R from the

scattering volume, the electric field of the wave scattered from the incident plane wave represented by Eq. 2.2 is given by [Villars and Weisskopf, 1955]

$$E_s = \frac{E_o K_o^2 \sin\psi}{4\pi R \varepsilon_o} \left| \int_V \delta\dot{\varepsilon}(\vec{r},t) \exp[i(\vec{K}_s - \vec{K}_o)\cdot\vec{r}]\, dV \right| , \quad (2.13)$$

where $\vec{r}$ is the radius vector from the origin of the coordinate system, ψ is the angle between the electric field vector of the incident wave and the direction of the scattering, and $\vec{K}_s$ is the wave vector of the scattered radiation. The wave vectors from waves scattered at different points within the scattering volume are almost identical because the scattered field is calculated for a point far from V.

The average power scattered per unit solid angle can be written as

$$\left\langle \frac{dP}{d\Omega} \right\rangle = R^2 \left\langle |E_s|^2 \right\rangle . \quad (2.14)$$

Then from Eq. 2.5 the differential scattering cross section per unit volume is

$$\frac{d\sigma_V}{d\Omega} = \frac{R^2 \left\langle |E_s|^2 \right\rangle}{V E_o^2} \quad (2.15)$$

Substituting for $|E_s|$ from Eq. 2.13, we get

$$\frac{d\sigma_V}{d\Omega} = \frac{K_o^4 \sin^2\psi}{(4\pi)^2 \varepsilon_o^2} \left\langle \left| \int_V \delta\varepsilon(\vec{r},t) \exp[i(\vec{K}_s - \vec{K}_o)\cdot\vec{r}]\, dV \right|^2 \right\rangle . \quad (2.16)$$

The dielectric constant at frequencies which are much higher than the plasma frequency ω_p is given by:

$$\varepsilon = \varepsilon_o \left(1 - \frac{\omega_p^2}{\omega_o^2} \right) \simeq \varepsilon_o , \quad (2.17)$$

where ε_o is the permitivity of free space and

$$\omega_p^2 = \frac{ne^2}{m\epsilon_o} \quad . \tag{2.18}$$

If the electron density is written as

$$n = n_o + \delta n(\vec{r},t) , \tag{2.19}$$

then the deviation of the dielectric constant from its mean value is

$$\delta\epsilon(\vec{r},t) = - \left(\frac{e^2}{m\omega_o^2}\right) \delta n(\vec{r},t) \quad . \tag{2.20}$$

The deviation of the density from its mean value may be expanded in terms of its Fourier components in the volume V. Thus,

$$\delta n(\vec{k},\omega) = \int\int_V dV\, dt\, \exp(i\vec{k}\cdot\vec{r})\, \exp(i\omega t)\, \delta n(\vec{r},t) \quad , \tag{2.21}$$

then

$$\frac{d\sigma_V}{d\Omega} = \frac{K_o^4 \sin^2\psi}{(4\pi)^2\epsilon_o^2} \left(\frac{e^2}{m\omega_o^2}\right)^2 \left| \left\langle \delta n(\vec{K}_s - \vec{K}_o, \omega) \right\rangle \right|^2 \quad . \tag{2.22}$$

This result is entirely general; it may be used to obtain the differential cross section for scattering from a turbulent plasma and from electron waves in a plasma, as well as from thermal density fluctuations.

From Eq. 2.22 it may be seen that the wavevector, $\vec{\kappa}_o = \vec{K}_s - \vec{K}_o$, of the density fluctuations responsible for scattering into the direction $\vec{K}_s$ must lie in the plane defined by $\hat{K}_s$ and $\hat{K}_o$. Electromagnetic scattering may thus be used to obtain the components of the velocity distribution of the particles.

The frequency spectrum of the scattered radiation is contained in the term $\left| \left\langle \delta n \right\rangle \right|^2$. Salpeter [1960a] has shown that the spectrum and intensity

of the radiation scattered from a thermal plasma depend on the dimensionless parameter

$$\alpha = \lambda_o/4\pi D \sin\frac{\theta}{2} \quad , \tag{2.23a}$$

where

$$D = (\varepsilon_o kT_e/N_e e^2)^{1/2}, \tag{2.23b}$$

is the well known Debye length. This is the minimum distance over which collective effects between the electrons and the ions may take place. The dependence of α on the electron temperature T_e and the electron density N_e is shown in Fig. 2.1. The differential scattering cross section may be written [Salpeter, 1960a,b]

$$\frac{d\sigma}{d\Omega} = r_e^2 \sin^2\psi \left\{\frac{\Gamma_\alpha(x)}{\omega_e} + Z\left(\frac{\alpha^2}{1+\alpha^2}\right)^2 \frac{\Gamma_\beta(y)}{\omega_i}\right\} \quad , \tag{2.24}$$

where

$$\omega_e = [2\kappa_o^2 kT/m]^{1/2} \tag{2.25a}$$

$$\omega_i = [2\kappa_o^2 kT/M]^{1/2} \tag{2.25b}$$

$$\beta = \alpha(1+\alpha^2)^{-1/2} \tag{2.25c}$$

$$x = (\omega - \omega_o)/\omega_e \tag{2.25d}$$

$$y = (\omega - \omega_o)/\omega_i \ . \tag{2.25e}$$

Γ is a function of the form

$$\Gamma_\gamma(z) = \exp(-z^2)\{[1 + \gamma^2 - \gamma^2 f(z)]^2 + \pi\gamma^4 z^2 \exp(-2z^2)\}^{-1}, \tag{2.26}$$

where

$$f(z) = 2z \exp(-z^2) \int_0^z \exp(t^2)\, dt. \tag{2.27}$$

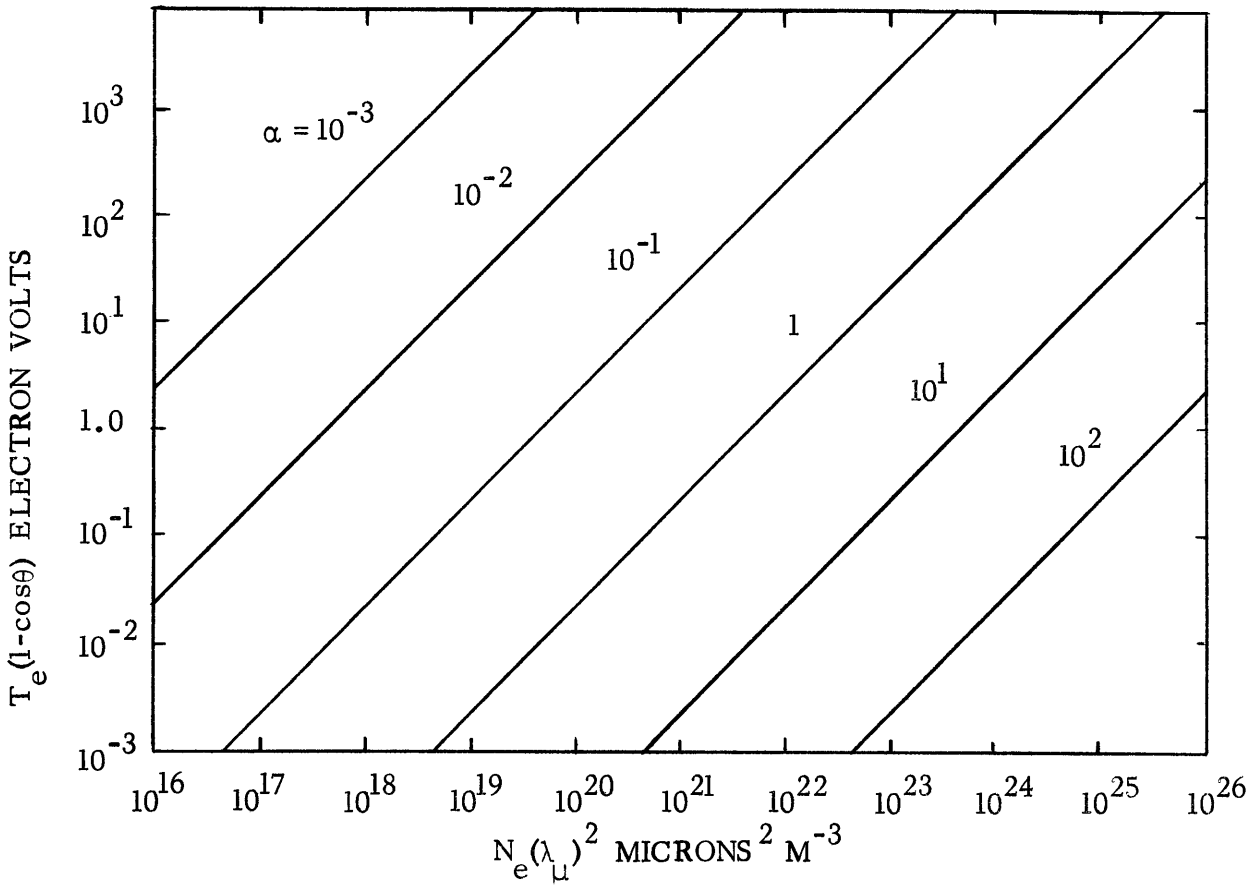

Fig. 2.1. Lines showing constant α vs electron temperature T_e and density N_e for scattering of 1 micron radiation at 90^o. The coordinates may be scaled as shown to obtain α for different incident wavelengths and scattering angles. (From Gerry, 1965a).

$\Gamma_\alpha(x)$ was plotted by Salpeter [1960a] for various values of α, and is shown here for reference in Fig. 2.2. For $\alpha << 1$, the first term in Eq. 2.24 is the dominant term. The spectrum is then a Gaussian whose width is the Doppler width associated with the electron thermal velocity.

For $\alpha > 1$, the function $\Gamma_\alpha(x)$ has a sharp maximum near $x = \pm x_o$, where x_o is a solution of the equation

$$f(x_o) - 1 = \alpha^{-2}. \tag{2.28}$$

$\Gamma_\alpha(x)$ has an approximately Lorentzian shape near x_o. If Eq. 2.28 is solved approximately by using the first two terms of the expansion for $f(x) - 1$, the result is [Salpeter, 1960a]

$$x_o^2 \simeq \frac{1}{2}(\alpha^2 + 3), \tag{2.29}$$

or rewritten

$$(\omega - \omega_o)^2 = (x_o\omega_e)^2 \simeq \omega_p^2 + 3kT\kappa_o^2/m. \tag{2.30}$$

This is the dispersion equation for longitudinal plasma oscillations. Physically, then, these satellite peaks are associated with the creation and destruction of electrostatic plasma oscillations. For $\alpha > 1$, the second term on the right in Eq. 2.24 represents a narrow central peak which arises from collective effects between the ions and electrons. Its width is approximately the Doppler width associated with the ion thermal velocity. Its shape is discussed in detail by Salpeter [1960a].

The total scattered intensity is obtained by integrating Eq. 2.24 over all frequencies. The result is

$$\sigma_t = r_e^2 \sin^2\psi\{(1 + \alpha^2)^{-1} + Z\alpha^4(1 + \alpha^2)^{-1}[1 + (Z+1)\alpha^2]^{-1}\}. \tag{2.31}$$

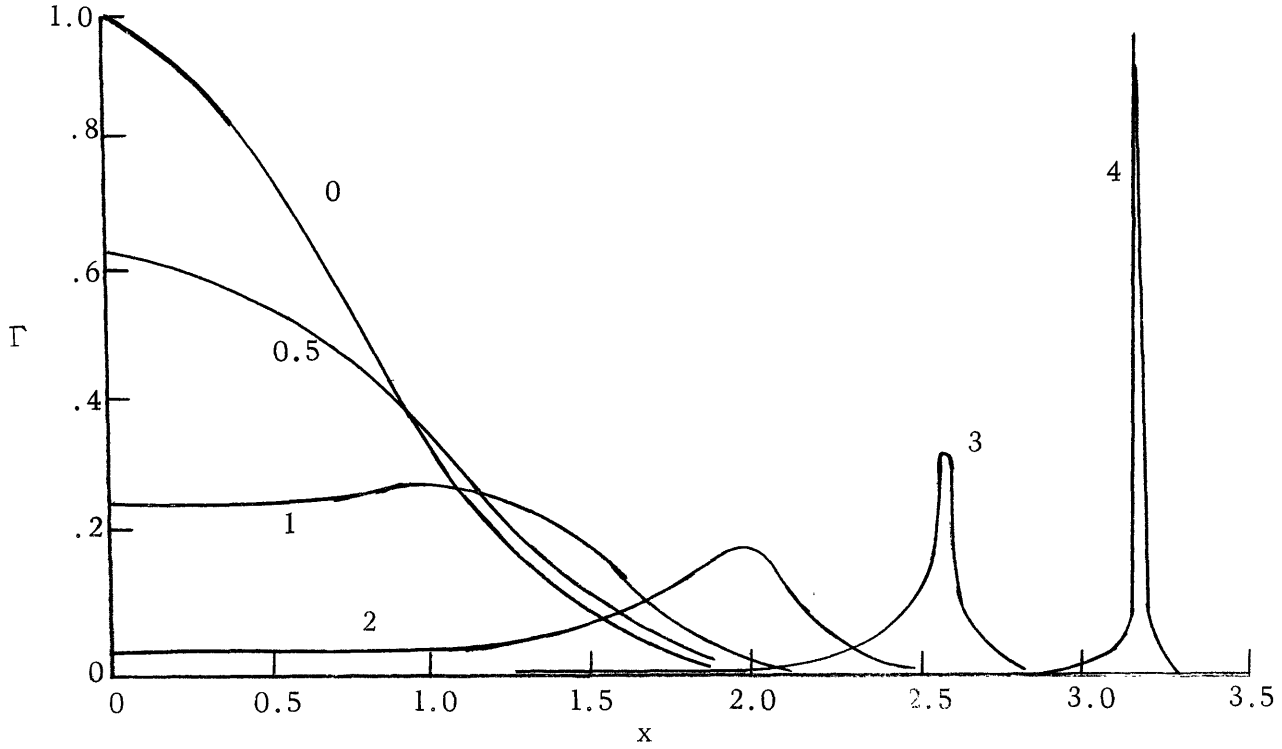

Fig. 2.2. The function $\Gamma_\alpha(x)$ plotted against x for α = 0, 0.5, 1, 2, 3, and 4. (After Salpeter [1960-1]).

The first term is referred to as the electron component, the second as the ion component.

C. Scattering from Nonequilibrium Plasmas

A nonequilibrium situation occurs when the components of the velocity distribution of a species are Maxwellian, but each component has a different temperature (defined in this case by Eq. 2.11) associated with it. This might be expected to occur in a plasma in a magnetic field, if energy is added to the particles only in a direction parallel to the field lines. Since the components of the velocity distribution can be obtained from scattering measurements, it is possible to ascertain if such an asymmetry is present in a given plasma.

Another case of a nonequilibrium plasma is one in which an ion temperature T_i and an electron temperature T_e are defined but $T_i \neq T_e$. This case has been treated theoretically by Buneman [1962], Lambe [1962], Salpeter [1963], Moorcroft [1963], and Farley [1966]. Defining the following parameters:

$$\alpha_e = \lambda_o/4\pi D_e \sin\frac{\theta}{2} \tag{2.32a}$$

$$\alpha_i = \lambda_o/4\pi D_i \sin\frac{\theta}{2} \tag{2.32b}$$

$$D_e = (\varepsilon_o kT_e/N_e e^2)^{1/2} \tag{2.32c}$$

$$D_i = (\varepsilon_o kT_i/N_i e^2)^{1/2} \tag{2.32d}$$

$$\omega_e = (2\kappa_o{}^2 kT_e/m)^{1/2} \tag{2.32e}$$

$$\omega_i = (2\kappa_o{}^2 kT_i/M)^{1/2} \tag{2.32f}$$

and

$$\beta = \alpha_i(1 + \alpha_i{}^2)^{-1/2} , \tag{2.32g}$$

the differential scattering cross section has the same form as Eq. 2.24 with

α replaced by α_e. Then the total cross section is

$$\sigma_t = r_e^2 \sin^2\psi[(1+\alpha_e^2)^{-1} + Z\alpha_e^4(1+\alpha_e^2)^{-1}(1+\alpha_e^2+\alpha_i^2)^{-1}]. \qquad (2.33)$$

The term in brackets was plotted by Buneman [1962], and is redrawn here in Fig. 2.3 for Z = 1 and various values of T_e/T_i. Moorcroft [1963] presents similar graphs for H^+ and O^+ plasmas.

D. Scattering from Plasmas in a Magnetic Field

For a thermal plasma it can be shown that a magnetic field alone can never alter the total scattered power [eg. Farley et al., 1961]. It merely redistributes the power over the spectrum. Thus, in the presence of a magnetic field, the total scattering cross section is still given by Eq. 2.31. The spectrum is again determined by the electron and ion density fluctuations. These have been written out explicitly by several authors [eg. Hagfors, 1961].

Considering only the regime $\alpha<<1$, if the scattering wave vector $\vec{K}_s$ is exactly perpendicular to the magnetic field vector $\vec{B}$, the spectrum consists of lines located at $\omega_o \pm n\omega_b$, for n = 0,1,2,..., where ω_o is the radian frequency of the incident radiation and ω_b is the gyrofrequency of the electrons. The fraction of the power contained in the two lines at $\omega_o \pm n\omega_b$ is [Laaspere, 1960]

$$\frac{\sigma_n}{\sigma_t} = \exp(-\xi) I_n(\xi) , \qquad (2.34)$$

where

$$\xi = \frac{kT\kappa_o^2}{m\omega_b^2} .$$

$I_n(\xi)$ is the modified Bessel function of the first kind of order n. The

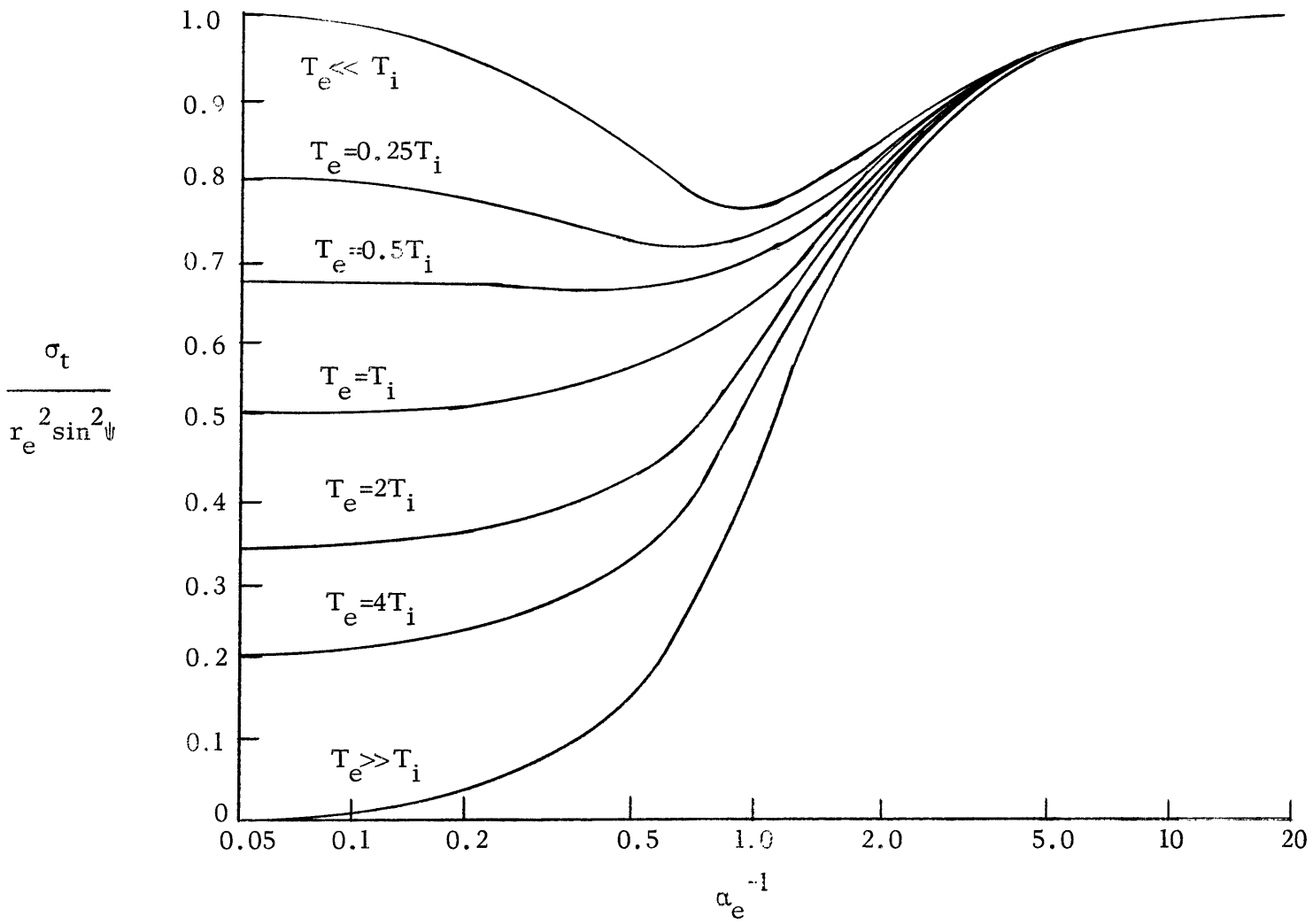

Fig. 2.3. The ratio of the total cross section to the Thomson cross section plotted vs α_e^{-1} for various values of T_e/T_i for a nonequilibrium plasma. (After Buneman [1962]).

envelope of these lines is the Doppler spectrum due to the electron thermal motion. The spectrum for the case $\xi = 6$ is shown in Fig. 2.4. If the angle between $\vec{\kappa}_o$ and $\vec{B}$ is different from zero, the spectrum is a superposition of Gaussians centered at each of the frequencies $\omega_o \pm n\omega_b$, for $n = 0,1,2,...$ The spectrum for $\xi = 6$, and $\phi = 5^o$ is shown in Fig. 2.5. This spectrum represents physically the creation and destruction of Bernstein [1958] waves within the plasma.

For a nonequilibrium plasma in a magnetic field, the total scattered power is not independent of the magnetic field [Farley, 1966].

E. Nonlinear Scattering Phenomena at High Radiation Intensities

Many authors have presented theoretical calculations of the cross section for nonlinear scattering effects. At high radiation intensities, the electric field of the incident radiation will drive damped plasma waves. A second radiation field may then be used as a probe to scatter from these waves. In the literature, this has been termed a light-off-light scattering experiment. The spectrum of the scattered light consists of linear combinations of the incident frequencies [Salat, 1966; Kroll et al., 1964; Berk, 1962; Platzman et al., 1964b; and Fried and Frank, 1963a]. When the frequency difference approaches the plasma frequency, the intensity of the scattered radiation increases and the spectrum is given by the ion density fluctuations. These effects are only observed when the wave vectors of the incident fields are parallel. A single radiation field may also scatter from its self-induced plasma waves. This will produce scattered radiation at the harmonic frequency $2\omega_o$ with a wave vector $2\vec{K}_o$ [Salat and Schlüter, 1965].

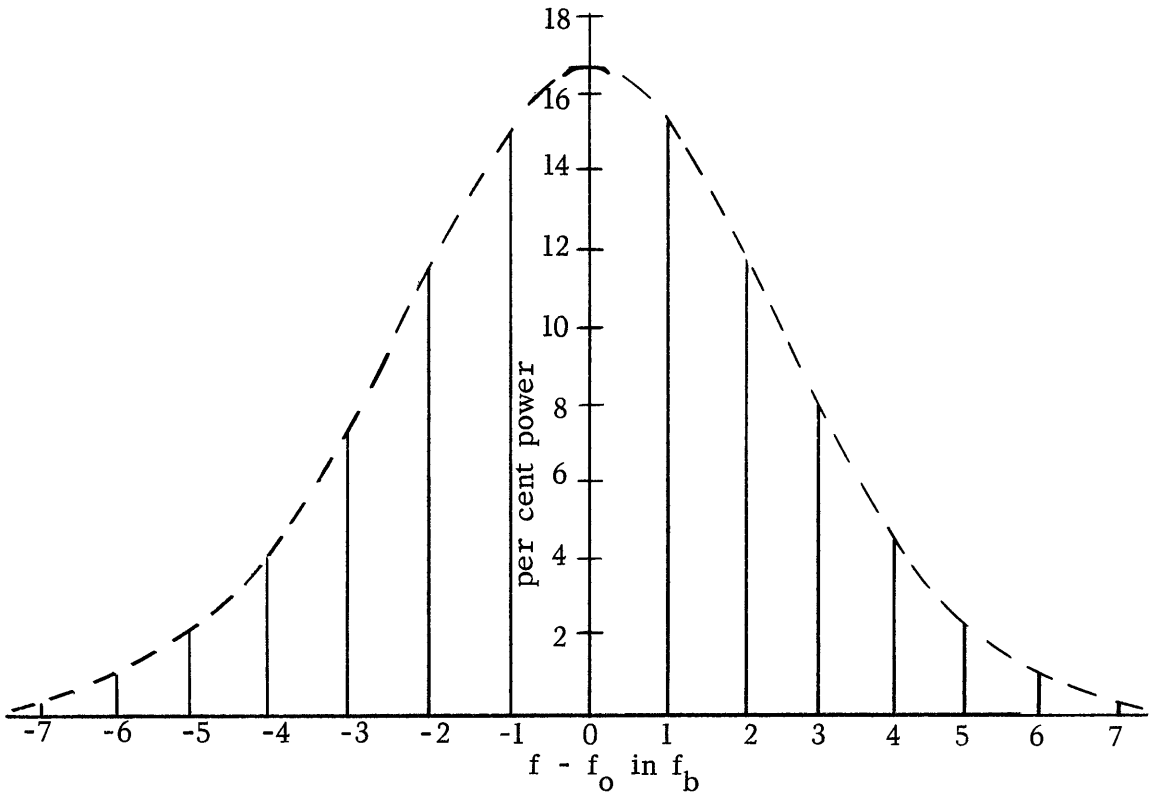

Fig. 2.4. Spectrum of backscatter with $\xi = 6$, $\varphi = 0^{o}$. Dashed line gives the Gaussian Doppler-shift spectrum for no magnetic field. (After Laaspere [1960]).

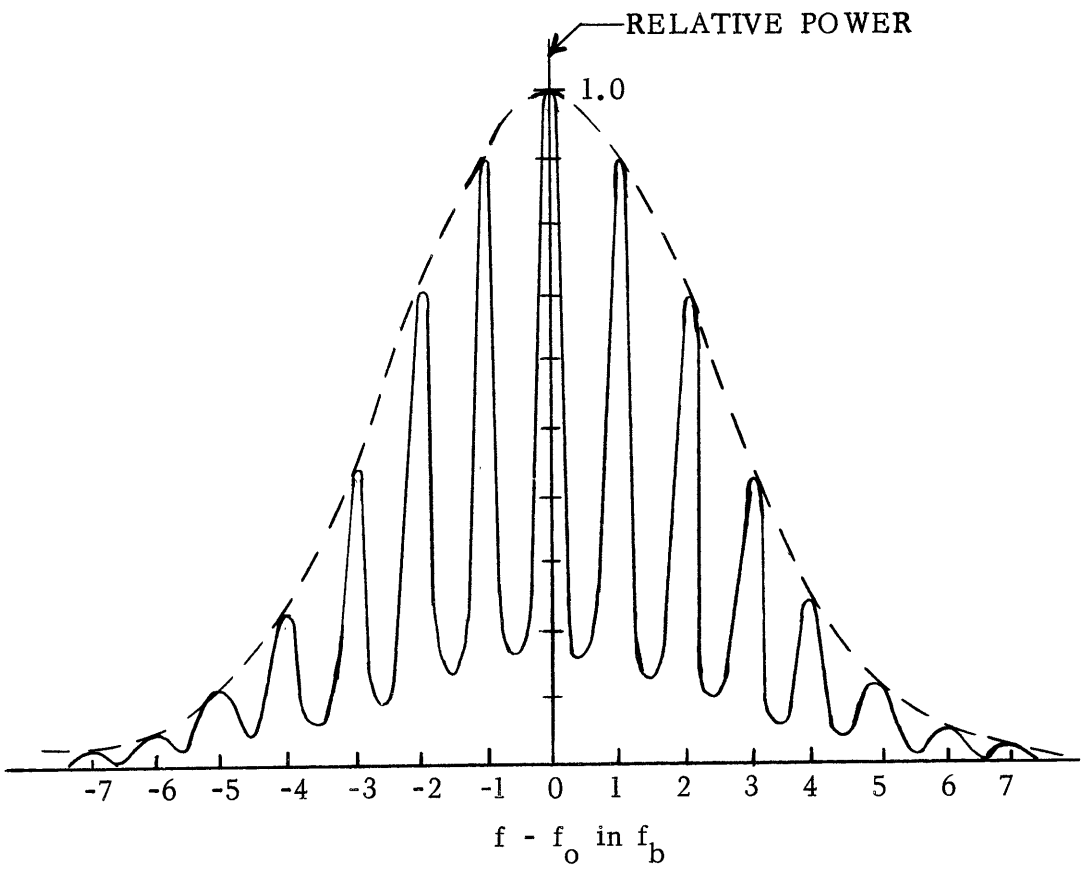

Fig. 2.5. Spectrum of backscatter with $\xi = 6$, $\varphi = 5^{o}$. (After Laaspere [1960]).

Baym et al. [1966] have shown that the light-off-light scattering cross section can never be as large as the cross section for incoherent scattering. They show that at stronger incident fields, stimulated Raman scattering is the dominant scattering mechanism. Kegel [1965] has considered the problem of forced density fluctuations in a plasma in a magnetic field. The appropriate dispersion relation is then the Bernstein relation. Again the scattered light contains the sum and difference frequencies of the incident waves.

Rosen [1959] has shown that Bragg reflection of electromagnetic waves from longitudinal plasma oscillations is possible. The scattering angle is obtained from the Bragg relation,

$$\tilde{\lambda} = \lambda_o/2 \sin \frac{\theta}{2} \quad , \tag{2.35}$$

where $\tilde{\lambda}$ is the longitudinal plasma wavelength, and λ_o is the wavelength of the incident radiation. Using the plasma dispersion relation,

$$\tilde{\omega}^2 = \omega_p^2 + 3kT\tilde{K}^2/m \quad , \tag{2.36}$$

the scattering angle is obtained from

$$\sin^2 \frac{\theta}{2} = \frac{\lambda_o^2[(\tilde{\omega}/\omega_p)^2 - 1]}{48\pi^2 D^2} \quad , \tag{2.37}$$

where D is the electron Debye length.

Ivanov and Ryutov [1965] have also discussed scattering from plasma oscillations in a plane plasma layer under the assumption that the wavelength of both the incident and the scattered radiation is large compared to the thickness of the layer. They discuss the possible use of scattering for a direct experimental verification of the existence of strong

fluctuations in a turbulently heated plasma.

Multiple photon processes have been considered by Fried [1961, 1963b], Mandel [1964], and Stehle [1963]. In general, it is found that all such effects are too small to observe at currently available pulsed laser intensities.

Pappert [1963] has considered relativistic effects on the scattering cross section. The significant parameter is found to be β_e, the square root of the ratio of the electron temperature to the rest mass energy of the electron. To the first order in β_e, the total cross section remains unaltered. However, an asymmetry in the spectrum about ω_o does occur.

Vachaspati [1964] has shown that the frequency of the light scattered by a free electron depends on the intensity as well as the wavelength of the incident radiation. Also, shifts are observed in the phases of the fundamental wave and the harmonic. These effects are enhanced if a large number of successive light pulses fall on the electron. He discusses the possibility of experimentally detecting the phase change by interference experiments using a ruby laser as the radiation source. High intensity effects have also been discussed by Mizushima [1963] and by Brown and Kibble [1964].

Theimer [1966] has shown that high density corrections to the scattering cross section are required if the number of electrons in a Debye sphere falls below 0.5.

CHAPTER III

REVIEW OF PREVIOUS EXPERIMENTS

A. Geophysical Experiments

The first experiment in which electromagnetic radiation scattered from a plasma was successfully observed was reported by Bowles [1958]. Using a 41 MHz radar pulse transmitter and receiver operating at a peak-pulse power of 4 to 6 x 10^6 Watts with a pulse width from 50 to 150 x 10^{-6} sec, he observed a rise in power-received peaking broadly at about an altitude of 350 km. He interpreted this as semi-incoherent scatter by the free electrons in the ionosphere. The line width was considerably smaller than the width expected from Doppler broadening due to the electron's thermal motion. This result may be understood theoretically from a calculation of the scattering parameter α. Assuming that the electron density at the peak of the F2 region is about 10^{12} m^{-3} and their temperature is 1000 ^oK, the value of α for the backscatter at 41 MHz is 270. This is very much greater than one, so that the spectrum is determined by collective effects between the ions and electrons. The line width would then be that associated with the ion thermal motion not the electron thermal motion.

Pineo et al. [1960a] reported backscatter observations at 440 MHz. They were able to obtain returns up to an altitude of 800 km. They also measured the frequency spectrum from returns from about 315 km. The observed spectral width was roughly 5% to 10% of that predicted on the basis of Doppler broadening by the thermal motion of the electrons.

One of the first important geophysical measurements was reported by

Van Zandt and Bowles [1960]. A plot of the scattered intensity vs. altitude indicated an exponential decrease of electron density between 370 km and 520 km. The logarithmic decrement deduced from the data lead to a temperature of 1050 ± 90 ^{o}K. This agrees well with other temperature determinations for the F-region.

Pineo et al. [1960b] reported measurements of the relative widths of returns from the E and F-regions. These indicated that the E-region temperature is five times lower than the F-region temperature. They also obtained the diurnal variation of the height of the maximum F-region backscatter at 440 MHz.

Detailed diurnal variations of the spectral characteristics were reported by Pineo et al. [1962]. The spectral widths indicated average night and day ion temperatures of about 650 ^{o}K and 1200 ^{o}K respectively. The observed spectral shapes were in general agreement with theoretical calculations for backscatter from a nonequilibrium plasma ($T_e \neq T_i$) in the absence of a magnetic field.

Perkins et al. [1965] have observed the plasma satellite lines in ionospheric backscatter. The received power was averaged over 4.8×10^4 pulses. The values of α calculated from the data ranged from 7 to 12.

All of the experiments that have been reported were operating in the regime $\alpha >> 1$. With present high power radars operating at centimeter wavelengths, it is possible to reach values of α which are less than one. For example, operating at a wavelength of 2.0 cm and backscattering from a region where the electron density is 5×10^{11} m^{-3} and the temperature is 1200 ^{o}K, the value of α is about 0.4. If the wave vector of the radar pulse is nearly perpendicular to the magnetic field vector in the F-region,

backscattered radiation should have a line spectra such as the one described in Section II-D. The separation in frequency between the lines is the electron gyrofrequency,

$$f_b = \frac{eB}{2\pi m} . \qquad (3.1)$$

If B is 0.5 Gauss, f_b is 1.4 MHz. The spectral width of the envelope of these lines is roughly the electron Doppler width. This may be calculated from Eq. 2.11. At a wavelength of 2.0 cm and an electron temperature of 1200 ^{o}K, the full width at half-height is 48 MHz. Such an experiment might be a means of observing the effect of a magnetic field on the spectrum of scattered radiation.

B. Pulsed Ruby Laser Experiments

The first laboratory laser scattering experiment was reported by Fiocco and Thompson [1963a]. They detected photons scattered from a ruby laser beam at 6943 Å by electrons in a 100 mA, 2 kV electron beam. The large Doppler shift associated with such a high energy eliminated the problem of background radiation from the laser. The electron density was 5×10^{15} m^{-3}. Thompson and Fiocco [1963a,b] were also the first to observe scattering of laser radiation from a laboratory plasma. For this experiment they used a hollow cathode discharge as the plasma source and found the electron temperature to be about 3 eV.

Additional features of the spectrum of the radiation scattered from a plasma were observed in later experiments by other investigators. Davies and Ramsden [1964] were the first to obtain good spectral resolution in the regime $\alpha \ll 1$. Kunze et al. [1964a] observed the satellite peaks near $\alpha = 1$. They were, however, unable to resolve them. Ascoli-Bartoli et al.

[1965] resolved the central ion line and the satellite peaks with a Fabry-Perot interferometer. They were able to determine both the electron and the ion temperature from the scattering data taken at $\alpha = 2$. Kronast et al. [1966] observed an asymmetric ion peak in a θ-pinch plasma. The ion temperature was found to be 108 eV and the electron temperature, 45 eV. They attributed the asymmetry to strongly excited plasma waves such as those discussed by Rosenbluth and Rostoker [1962]. A similar asymmetry was also observed by Evans et al. [1966b]. Daehler and Ribe [1967a] obtained a very well resolved spectrum of the central peak at $\alpha = 1.2$. The spectrum showed an intense narrow central peak, with broad wings whose width and magnitude corresponded to the theoretically expected thermal ion feature. The central peak had a magnitude 15 times greater than that of the theoretical ion feature and was 0.44 times as wide. They attributed this central peak to superthermal plasma density fluctuations.

If the parameter β, defined after Eq. 2.24, becomes $\simeq 1$, the ion line will develope satellites at

$$\Delta\omega = [\omega_{p+}^2 + 3kT_+\kappa_o^2/M]^{1/2}. \tag{3.2}$$

These ion wings have been observed by Weichel et al. [1967].

A list of the papers reporting experiments that have been performed with a pulsed ruby laser as the radiation source is given in Table 3.1. These experiments have verified in detail the theoretical results presented in Chapter II for both equilibrium and nonequilibrium plasmas. No effects due to the presence of a magnetic field have been reported. Deviations between the experimental results and the theory can, for the most part, be attributed to either scattering from coherent plasma waves or from bulk

motions of the plasma.

C. Continuous-wave Laser Experiments

The only cw laser scattering experiment that has been reported in the literature is an experiment by Farrow and Buchsbaum [1965]. They placed a hot-cathode discharge in helium within the cavity of a He-Ne laser, and used a synchronous detection system to reduce background noise. It was not clear that Thomson scattering was actually observed. The percent ionization in the plasma was 3.5×10^{-6}. Hence, Rayleigh scattering from the ground state helium atoms would be at least ten times larger than the Thomson scattering. Also, the scattered spectrum was not significantly broader than the resolution of the monochromator used.

D. Microwave Scattering Experiments

Nonlinear frequency mixing in a plasma is most easily observed at microwave frequencies. The cross section is greatly enhanced when the frequency difference between the two incident waves is equal to a resonant frequency of the plasma. Stern and Tzoar [1965] reported observing microwave scattering at a plasma resonance from electron plasma oscillations generated in a laboratory discharge. The scattering cross section was enhanced by exciting Tonks-Dattner oscillation modes. Two microwave signals were beamed at the plasma. One was a high frequency signal, $f_{inc} = 10.5$ GHz, the other was a low frequency signal, $f_p = 2.6$ GHz, which could excite a Tonks-Dattner mode. Scattered radiation was observed at the difference frequency, $f_{sc} = 7.9$ GHz.

Stern [1965] has also observed the generation of a second harmonic while illuminating a plasma with a 4 GHz signal. The second harmonic

occured only at electron resonances.

Wada [1967] and Wharton and Malmberg [1967] have also reported microwave scattering from plasma waves.

Table 3.1 The plasma parameters used in experiments that have been performed with pulsed ruby lasers.

AUTHORS	N_e	T_e	T_i	α
Anderson [1966]	$2.2 \times 10^{16} cm^{-3}$	2.0 eV		1.4
Ascoli-Bartoli et al. [1964b]	3.2×10^{15}		70 eV	> 1
" " " [1965]		70	70	> 1
Chan and Nodwell [1966]	6.3×10^{16}	1.2		4.4
Consoli et al. [1966]	2.2×10^{15}	2.3		0.3
Daehler and Ribe [1967a,b]	2.8×10^{16}	345	2×10^3	1.2
Davies and Ramsden [1964]	5×10^{15}	3.3		< 1
De Silva et al. [1964]	9×10^{14}	2.2		<< 1
" " " [1965]		2.2		0.15; 1.7
Evans et al. [1966a,b]				1.2-1.5
Fiocco and Thompson [1963a,b]	5×10^9	2×10^3		
Funfer et al. [1963a]	10^{17}			
Gerry [1965b]	5×10^{13}	1.0		
Gerry and Rose [1966]	10^{13}-10^{14}	3-8		< 1
Izawa et al. [1966]	10^{16}	few		0.85
Kronast et al. [1966]	6×10^{16}	45	108	$\beta = 0.65$
Kunze et al. [1964a]	$2\text{-}4 \times 10^{16}$	4.7-7.8		0.53-1.0
" " [1964b]	$10^{16} - 10^{17}$	20-50		

Table 3.1 Continued.

AUTHORS	N_e	T_e	T_i	α
Kunze et al. [1965a]		134-215		<< 1
Patrick [1965]	10^{15}-10^{17}	20-100		< 1
Patrick and Gerry [1965]	4-10 x 10^{15}			
Ramsden and Davies [1965]	5 x 10^{19}		$\leq$ 10	> 1
" " [1966]	2.4 x 10^{15}	1.1		0.5; 3.0
Ramsden et al. [1966]	2 x 10^{17}	800	200	3
" " [1967]	1.4 x 10^{17}	80	300	
Schwarz [1965]	10^{14}			
Sigman et al. [1965]	10^{13}			
Thompson and Fiocco [1963a,b]	10^{13}	3		
Weichel et al. [1967]	10^{19}	25		7

CHAPTER IV

EXPERIMENTAL CONSIDERATIONS

A. Plasma Scattering Experiments in General

1. The Radiation Source

The radiation source used in a plasma scattering experiment must have several specific characteristics. First, it must be high powered because the Thomson cross section is extremely small. In a typical experiment, roughly 10^{-15} of the incident power is scattered into the detector. The number of photons detected must be large enough to overcome the shot noise which is a fundamental limitation on the experiment. However, in practice, this is usually much smaller than the natural background noise from the plasma. This background radiation consists of Brehmsstrahlung continuum from free-free transitions within the plasma and spectral lines within the passband of the detector. Gerry [1965a] has shown that the signal-to-noise ratio is independent of the electron density if continuum radiation is the dominant source of noise.

Second, the radiation should be well collimated if one wishes to measure the plasma parameters in a small volume. A well collimated beam maximizes the incident energy falling on the scattering volume and allows one to limit the background radiation to that coming from a smaller volume. In practice, this may be as small as a few cubic millimeters if a high powered laser is used.

Because of the high power required, optical scattering experiments were not practical before the advent of the laser. The wavelengths are limited

to those at which lasers are available. It is advantageous to use wavelengths near the peak of the quantum efficiency of available photomultipliers. For an S-20 surface, the peak is about 20% near 5000 Å. Unfortunately, the pulsed ruby and neodymium lasers operate in the near infrared where the quantum efficency available is only one or two percent.

The wavelength also determines the value of the scattering parameter α at fixed plasma parameters and scattering angle. In this instance, a longer wavelength is desirable to reach the condition $\alpha > 1$, at which collective effects can be observed. The continuous-wave CO_2 lasers currently becoming available operate at a principle wavelength of 10.6 microns and are thus well suited to operate at $\alpha > 1$.

Finally, the incident radiation should be nearly monochromatic in order that small Doppler shifts can be observed. This is particularly necessary in the regime $\alpha > 1$, where the line is broadened by ion motions. It may be advantageous to single-mode the laser in this regime.

2. Other Interactions of the Laser Radiation with the Plasma

Free-free absorption of the laser beam may cause a significant heating of the plasma electrons. Gerry [1965a] has calculated the energy increase per electron as a function of the energy flux of the incident radiation. A plot of his results is reproduced in Fig. 4.1. The increase is negligible at the power levels used for the Ar^+ scattering measurements reported in this thesis.

Bound-free absorption may cause an increase in the electron density, resulting in an increase in the background radiation. This is most likely to occur in plasmas with a low degree of ionization. Such a broad-band

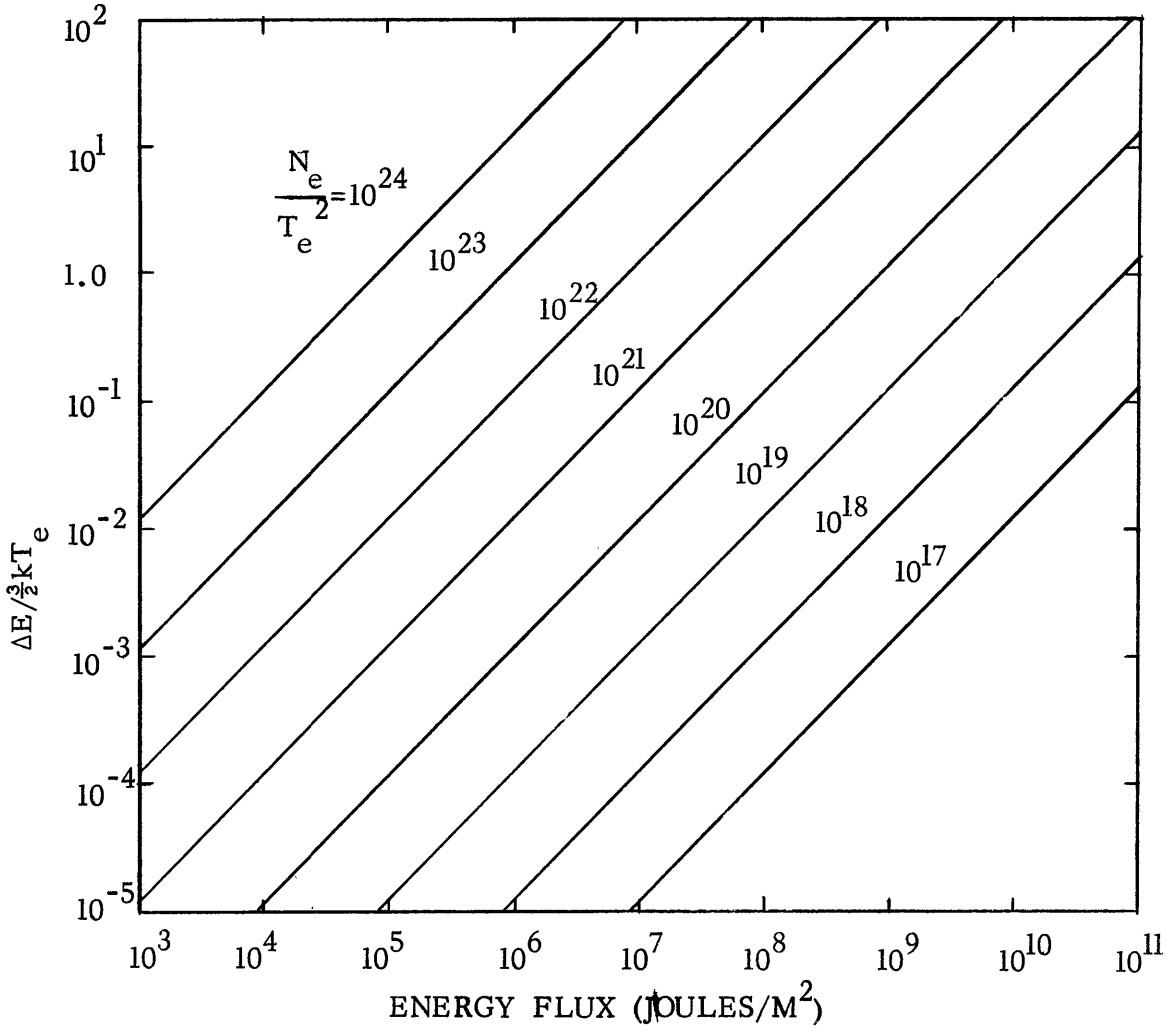

Fig. 4.1. Graph showing the fractional electron energy increase due to absorption of laser energy. The parameter is electron density divided by the square of the electron temperature in volts. (After Gerry [1965a]).

light increase has been observed by Lidsky et al. [1964]. They observed a time-delayed signal following a Thomson-scattered signal from a ruby laser pulse. The delayed signal was independent of wavelength over 500 Å and it was unpolarized. They suggest that this anomalous radiation follows photoionization of excited neutral atoms.

Raman and Rayleigh scattering from neutral atoms, molecules, and ions may compete with Thomson scattering. In Raman scattering, a change of state takes place in an atom or molecule and the frequency of the incident photon is changed by an amount corresponding to the energy difference between the initial and the final state. The rotational Raman spectra of light, scattered from diatomic molecules or ions, can produce scattering over many Ångstroms on either side of the incident wavelength. Although Raman cross sections are considerably smaller than the Thomson cross section, this problem is best dismissed by choosing a monatomic gas for the experiment. Excited molecules and molecular ions in the plasma may have large Raman cross sections.

The differential scattering cross section for Rayleigh scattering at 4880 Å for common gases is shown in Table 4.1. Although the cross section for all of these gases is smaller than that for Thomson scattering, Rayleigh scattering would dominate Thomson scattering in a weakly ionized gas. In the regime $\alpha << 1$, the two could be easily distinguished because the Doppler width of the Rayleigh scattered radiation would be that corresponding to the temperature of the neutral atoms, while the Doppler width of the Thomson scattered radiation would be that corresponding to the temperature of the electrons. In the regime $\alpha > 1$, they could not be so distinguished since both are Doppler broadened by the neutral (or ion) temperature.

Table 4.1 The differential Rayleigh scattering cross section at λ_o = 4880 Å and $\psi = 90^o$ for some common gases. The differential Thomson cross section is included for comparison.

Gas	Differential Rayleigh Cross Section
e^- (Thomson)	8.0×10^{-30} m^2
He	1.2×10^{-33}
Ne	4.3×10^{-33}
Ar	7.6×10^{-32}
Kr	1.7×10^{-31}
Hg	8.5×10^{-31}
Air	8.1×10^{-32}
H_2	1.9×10^{-32}
O_2	7.1×10^{-32}
N_2	8.7×10^{-32}
H_2O	6.0×10^{-32}

Helium is the best choice to minimize Rayleigh scattering and to eliminate vibrational and rotational Raman scattering.

3. Reduction of Background Light

Because the incident power is much smaller than the scattered power, scattering from the walls and other parts of the apparatus must be greatly reduced. Ideally, the interior walls should be optically black to absorb all of the radiation falling on them. Aluminum parts may be black anodised to a dull-black finish and brass may be black ebenoled.

Optical dumps should be used to dump the laser beam after it has passed through the scattering volume. Also, a viewing dump on the far side of the plasma, opposite the detector, will reduce radiation scattered from this wall directly into the detector. Gerry and Rose [1966] have discussed both materials and geometries suitable for such dumps.

Good quality lenses, mirrors, and windows should be used. Surface imperfections and bubbles in the glass will strongly scatter the laser radiation. The entrance window to the vacuum system should be placed as far as possible from the detector so that apertures can be placed between them to eliminate light scattered directly at the detector by this window.

Dust, as well as material sputtered from the electrodes,will also scatter large amounts of light from the beam. This may be responsible for the anomalously high scattered signals occasionally observed in ruby laser experiments.

Much of the plasma background may be eliminated by placing an interference filter, peaked at the laser line, in front of the detector. Since the plasma background is unpolarized while the laser radiation is approxi-

mately linearly polarized, a polaroid filter placed in front of the detector will increase the signal-to-noise ratio by about a factor of two.

B. Continuous-wave Experiments

In some experiments, cw laser sources may have several advantages over pulsed lasers. The output from a cw laser is, at present, considerably more stable and repeatable than that from a ruby laser. The wavelength at which a ruby lases depends on the temperature of the rod. Repeated firings tend to heat the rod, and can shift the output wavelength several Ångstroms. The wavelength stability and high degree of coherence available from cw lasers offers considerable advantages for narrow-band spectral analysis, which is necessary in measuring ion temperatures and observing collective effects. A cw source allows the use of counting or synchronous detection techniques. The latter may be used, for example, with a multichannel optical system to continuously monitor the electron density and temperature in a plasma device. If both the plasma density and the laser light are modulated and the scattered signal is detected at the sum or difference frequency, light scattered by the walls, windows, etc. as well as the plasma background will not be detected.

In a highly ionized plasma, density modulation may not eliminate Rayleigh or Raman scattering, since these depend on the ion and neutral densities which are also modulated along with the plasma current. Their cross sections are a thousand times smaller than the Thomson cross section. Thus, they may usually be neglected.

The power levels of the radiation from cw lasers are low, and the disturbance to the plasma is minimized. A factor of ten gain in power

may be realized by performing the experiment within the cavity of a cw laser.

Finally, wavelengths near the peak quantum efficiency of photocathodes are available from cw lasers. This is particularly true of the 4880 Å line from the argon ion laser. This line is near the peak of the quantum efficiency of the S-20 surface.

CHAPTER V

DESCRIPTION OF THE EXPERIMENT

The electron density and temperature in a low-density reflex discharge in helium were measured by observing the scattering of continuous-wave argon ion laser radiation at 4880 Å. A synchronous detection system was used to distinguish the weak scattered signal from the plasma continuum radiation, from spectral lines near 4880 Å due to impurities, and from the background laser light. The scattering measurements were made at an angle of approximately 8^{o} in two planes, one parallel and the other perpendicular to the magnetic field, as shown in Fig. 5.1. The spectrum obtained in the plane parallel to the magnetic field was determined by Doppler shifting due to electron velocities parallel to $\hat{B}$. The temperature measured in this plane will be referred to as $T_{\parallel}$. The spectrum obtained in the plane perpendicular to $\hat{B}$ was determined by Doppler shifting due to electron velocities perpendicular to $\hat{B}$. The temperature measured in this plane will be referred to as $T_{\perp}$. Both measurements were made in the regime $\alpha << 1$.

In this chapter, the reflex discharge, the laser, and the detection system are described. A schematic diagram of the experimental apparatus is shown in Fig. 5.2.

A. The Reflex Discharge Plasma Source

The reflex discharge was produced in a water-cooled, stainless steel vacuum chamber. The main cavity was a vertical cylinder 19.7 cm in diameter and 15.2 cm high. The metal chamber was the electrical ground for the

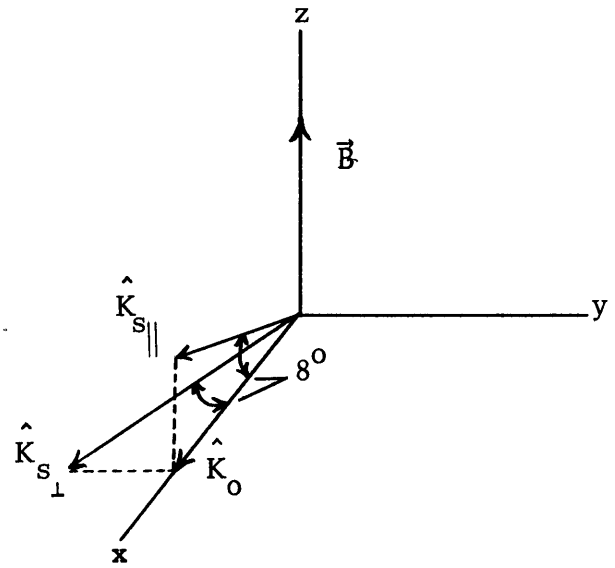

Fig. 5.1. Wave vector geometry for the scattering experiments.

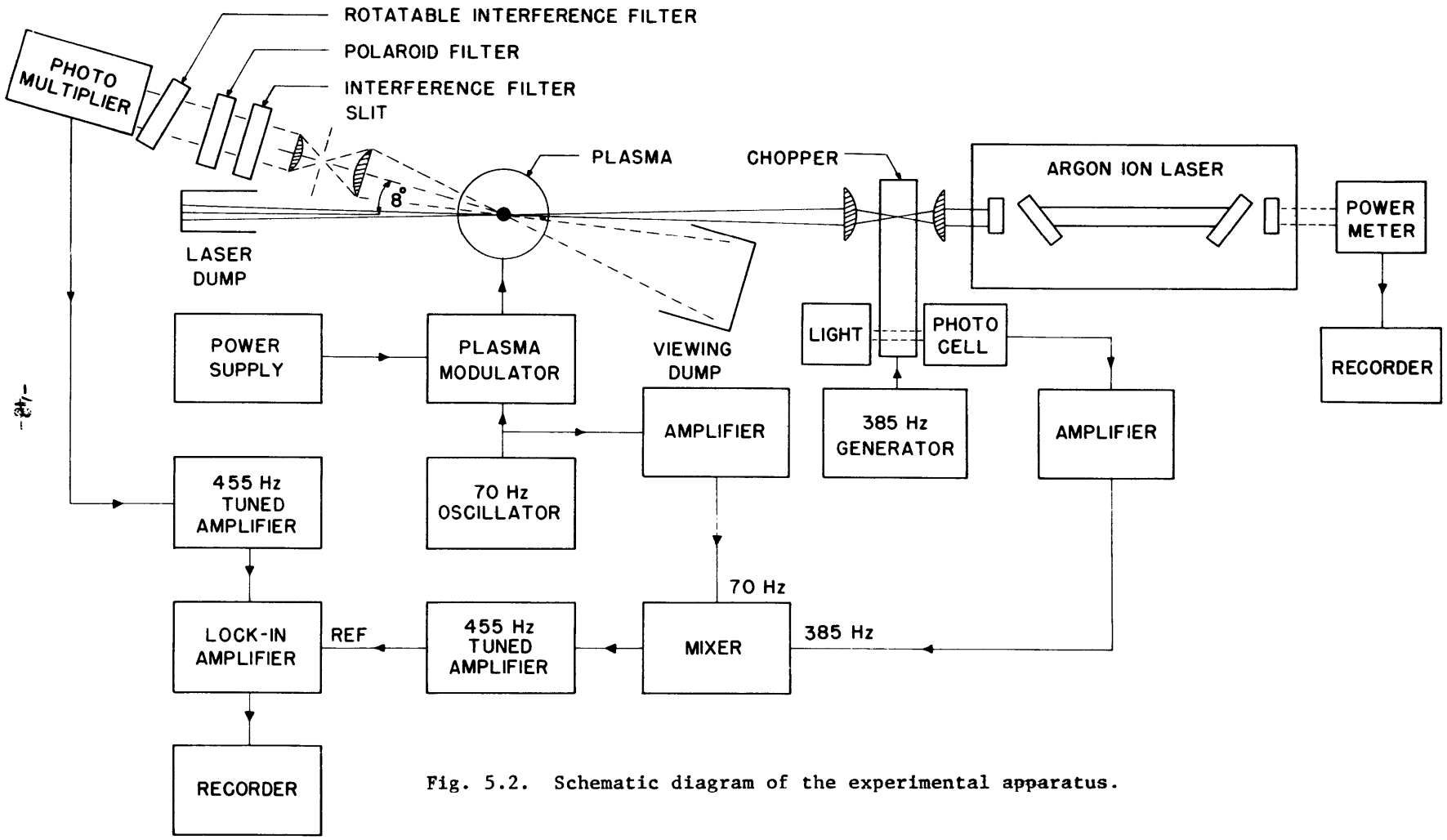

Fig. 5.2. Schematic diagram of the experimental apparatus.

system. Four ports, each with an inside diameter of 9.8 cm, were spaced evenly around the circumference of the cylinder. The electrodes were mounted through similar ports at the top and bottom, so that the anode rings were 7.5 cm apart and the cathodes about 16.3 cm apart along the axis of the cylinder. The electrode configuration is shown in Fig. 5.3. The anodes were hollow copper annuli 1.8 cm high, 3.8 cm inside diameter and 5.7 cm outside diameter. They were maintained at ground potential. The cathodes were coated tungsten spirals 5 mm od, 2.5 mm id, and 10 mm long. They were heated by a dc current between 2.5 and 3.0 Amps. They had a very short life — on the order of ten hours if the plasma discharge current ran over 2 Amps. The plasma was optically uniform for at least the first five hours, after which it broke up into filaments as hot spots formed on the cathodes. All of the data presented in Chapters VI and VII were taken under uniform conditions.

A metal plate at cathode potential prevented the discharge from going to the top and bottom plates of the vacuum chamber. A moderate magnetic field inhibited diffusion to the walls.

In between the large ports around the circumference of the vacuum chamber were four ports of 2.3 cm diameter. These were used for air inlets, the Langmuir probe, and viewing ports.

Pressure in the cavity was adjusted by setting the valve opening to the diffusion pumps, while maintaining a constant flow into the system through a Granville-Phillips vacuum valve. The ultimate pressure of the vacuum system was 2×10^{-6} Torr without a liquid nitrogen cold trap, and 4×10^{-7} Torr with the cold trap. It was normally run untrapped. The plasma was formed in helium at a pressure of 10^{-2} Torr. The pressure was measured

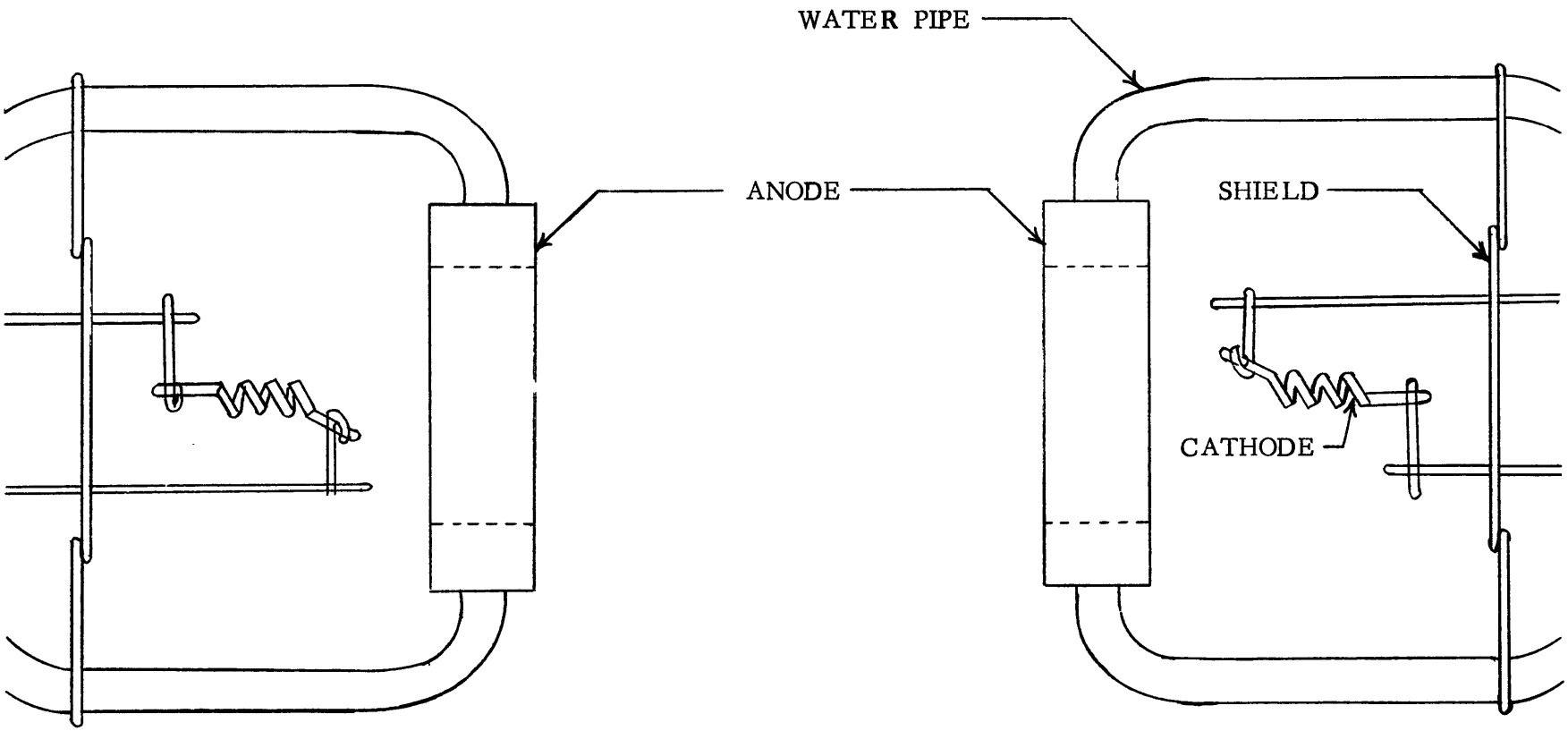

Fig. 5.3. Sketch of plasma electrode configuration. (Approximately to scale).

by a Pirani gauge, using the calibration for helium provided by the manufacturer. The average current through the discharge was typically 1.8 Amps. A set of Helmholtz coils provided an axial magnetic field of 0.1 Wb/m^2. The gas was then approximately 1% ionized at the center of the discharge.

The continuum and impurity line radiation from the plasma was considerably lower when the discharge was run with the pumps operating, compared to their value when it was run with the vacuum system sealed off. Grade A, pure, oil free, Navy helium was used for the gas. No difference was observed near 4880 Å between its radiation level and spectrum, and those of pure Airco helium.

The plasma current was modulated between 1.2 and 3.0 Amps for the purpose of synchronous detection. Fig. 5.4 shows a scope trace of a signal obtained from the plasma modulator. The vertical displacement is proportional to the current through the discharge. The "wings" are high frequency ($\sim$ 300 kHz) oscillations which occur in the indicated current range.

Radiation near 4880 Å from the helium plasma was scanned with a Jarrell-Ash Model 82-020 Scanning Spectrometer. The spectrometer was calibrated using the 4921.93 Å helium line. The impurity lines observed are shown in Table 5.1. The first is most likely the Ar II line corresponding to the same transition as the argon ion laser transition at 4879.9 Å.

The scattering experiment was first attempted by counting the number of photoelectrons produced by the photons incident on the photomultiplier. However, difficulties encountered in trying to eliminate the impurity line radiation led to the synchronous detection system. The background count from the plasma was about 100,000 counts per second within the

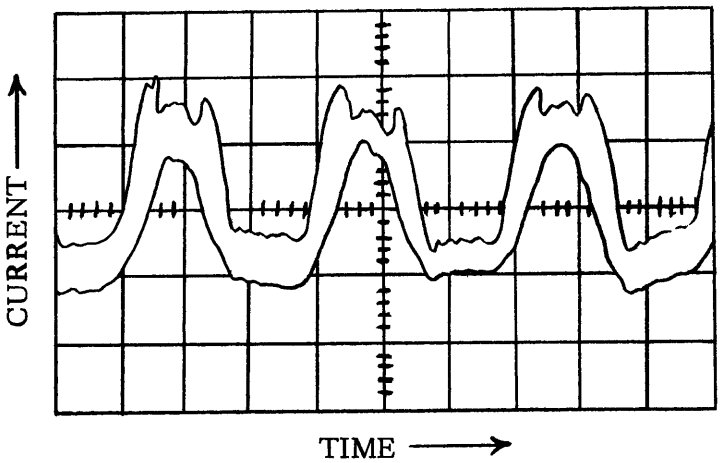

Fig. 5.4. Drawing from a picture of the scope trace of the signal from the plasma modulator. The vertical axis is proportional to the current through the discharge.

Table 5.1 Impurity lines near 4880 Å observed in the discharge.

Wavelength	Possible Identification	Relative Intensity
Continuum	---	750
4879.9	Ar II	8741
4876.0	Ar I	1388
4874.2	Ni I	1243
4873.1	Ar I or Ni I	2335

passband of the 1.58 Å interference filter. This radiation was unpolarized.

Measurements of the electron temperature and of the electron and ion densities were made by three different diagnostic techniques: helium line ratios, Langmuir probes, and cw laser scattering. The results of these measurements are described in Chapters VI and VII.

B. Argon Ion Laser

The Ar^+ laser was built by Spacerays, Inc. It had a total output power at several wavelengths of approximately 2.0 Watts. The power output at 4880 Å was typically 1.0 Watt. The optical cavity was 2.0 meters long. The water-cooled capillary was 1.0 meter long and 3 mm in diameter. At the end from which the output was taken, the cavity was terminated by a 90% reflecting mirror. The other end was terminated by a mirror of "maximum reflectivity" at 4880 Å. The output from this end was calibrated against the main output, and was continuously monitored while taking the measurements.

The Brewster angle windows were oriented so that the electric field vector of the radiation was in the horizontal plane. The angle between the scattering vector and the electric field vector was 82^o when measuring $T_\perp$ and 90^o when measuring $T_\parallel$.

The laser discharge was run at 425 Volts and 30 Amps. The argon pressure was approximately 0.2 Torr, and a slow gas flow from cathode to anode was maintained.

The width of the laser line was measured using a pressure-scanned Fabry-Perot interferometer, with a plate separation of 2 cm and a finesse of 20. The full width at half-height was 0.027 Å.

The output beam from the laser was focused by a 46 mm focal length

lens. Near the focal plane, the beam was chopped at 385 Hz by a vane attached to a synchronous motor. A second lens, with a 74 mm focal length, focused the beam near the center of the plasma column. Beyond the plasma, the beam entered a black anodised dump.

C. Optical Dumping Precautions

The light scattered by the plasma was extremely small compared to the background. The apparatus was designed to eliminate as much of this unwanted radiation as possible.

The lens which focused the laser beam at the center of the plasma was also used as the window of the vacuum chamber. This eliminated the need for an additional window which would have further scattered the laser light. This lens was placed 75 cm from the discharge. The intervening space contained anodised pipes, apertures, and baffels which prevented light scattered by the lenses from entering the detector.

A black anodised pipe, 38 cm long and 10.2 cm in diameter, was placed opposite the detector viewing lens for the $T_{\perp}$ measurement. It served as a background to eliminate direct scatter from the walls. Light entering this dump made a minimum of two reflections before returning to the main vacuum chamber. It was not used for the $T_{\parallel}$ measurement. A cone between the discharge and the viewing lens further reduced the background. By these means, the stray laser light entering the detector was about 5,000 counts per second compared to 100,000 counts per second from the plasma. This was still quite large compared to the expected Thomson scattered signal of less than 200 counts per second. Additional dumping might have further reduced the stray light. However, this was not necessary with the synchronous detection system.

D. Synchronous Detection System

A synchronous detection system was used to distinguish the weak scattered signal from the unwanted background radiation. For this purpose, the laser output was chopped at 385 Hz, and the current through the plasma was modulated between 1.2 and 3.0 Amps at 70 Hz. The scattered signal was detected at the sum frequency, 455 Hz.

Photons scattered from the laser beam, as well as those from the background radiation, were collected by a lens, 4.5 cm in diameter with a focal length of 10.5 cm, located at a distance of 42.2 cm from the center of the discharge. Radiation from the scattering volume was focused by this lens onto a 0.1 mm x 2.5 mm slit, which limited the field of view to an approximately rectangular cross section, 0.3 mm wide by 5.0 cm long, located along the incident beam at about the center of the plasma. Another lens collimated the light coming through the slit into an approximately parallel beam, which then passed through an interference filter, 20 Å wide, centered at 4880 Å; a polaroid filter; and a rotatable interference filter, 1.58 Å wide. The light was then detected by a 9558A EMI photomultiplier with a nominal quantum efficiency of 18% at 4880 Å and a gain of 1.8×10^6. The spectrum of the scattered light was obtained by rotating the narrow-band interference filter.

The photomultiplier output was amplified by a 1-Hz bandwidth amplifier tuned to the sum frequency, and then fed to a Princeton Applied Research HR-8 lock-in amplifier. Oscillator output at the component frequencies, 385 Hz and 70 Hz, were mixed across a diode. The sum frequency, 455 Hz, was used as the reference for the lock-in amplifier. The output of the lock-in amplifier was recorded as a function of time on a strip-chart recorder.

CHAPTER VI

PROBE AND SPECTRAL MEASUREMENTS

A. Electron Temperature and Density Determined from Langmuir Probe Measurements

1. Probe Theory

The following discussion of the simple probe theory follows Verweij [1960]. When the probe voltage is negative with respect to the plasma potential of the plasma immediately surrounding it, the probe repels electrons and attracts ions. A positive space charge layer builds up around the probe. However, the faster electrons can penetrate this positive layer. They produce an electron distribution given by Boltzman's law:

$$n = n_o \exp(eV/kT_e), \tag{6.1}$$

where n_o is the mean electron density within the plasma, and V is measured with respect to the plasma potential. The electron density at the surface of a probe held at a potential $-V_p$ with respect to the surrounding plasma is

$$n_s = n_o \exp(-eV_p/kT_e). \tag{6.2}$$

Assuming that all of the electrons striking the probe are collected, the electron current to a probe of area A is given by

$$i_e = \frac{1}{4} n_o e \bar{v} A \exp(-eV_p/kT_e), \tag{6.3}$$

where $\bar{v}$ is the average velocity of the electrons.

As the probe potential is changed from very negative to less negative

values, the positive ion current decreases while the electron current increases exponentially. At a certain negative value of the probe voltage, the electron current is equal to the ion current. This is called the floating potential. As the probe voltage is increased further, the probe current changes sign and the positive ion current becomes negligible with respect to the electron current, which continues to grow exponentially according to Eq. 6.3. In this region, the probe current is carried practically entirely by the electrons, so that Eq. 6.3 holds for the total probe current. Taking the logarithm of this equation, the following simple relation is found:

$$\ln i_e = - \frac{eV_p}{kT_e} + \text{const.} \tag{6.4}$$

Thus in the case of a Maxwell-Boltzmann velocity distribution for the electrons, the graph of the logarithm of i_e plotted as a function of the probe voltage (the reference potential may be arbitrary since it can be taken into the constant in Eq. 6.4) is a straight line over a certain region of the probe voltage. The electron temperature can be calculated from the slope S of this line:

$$T_e = - \frac{e}{kS} . \tag{6.5}$$

As the voltage is further increased, the electron current saturates due to spacecharge limitations on the current collected.

When a strong magnetic field is present, the electron saturation current is considerably reduced if the electron cyclotron radii are comparable to the probe dimensions. However, the slope at low probe current remains essentially unchanged, and may be used to determine the electron

temperature [Bohm et al., 1949].

Since the ion cyclotron radii are normally much larger than the probe dimensions, the ion saturation current is not seriously effected by the magnetic field. Bohm et al. [1949] have shown that the ion saturation current is a function of the electron temperature and of the ion density. It is given by

$$I_+ = 0.4\ n_+\ e\ A \left(\frac{2kT_e}{M_+}\right)^{1/2} . \qquad (6.6)$$

Since the ionization potential of helium is large, the predominant ion is the singly ionized helium ion. Thus the ion density and the electron density are the same, and Eq. 6.6 may be used to determine the electron density.

2. Description of the Probe Circuits

The probe consisted of a 40 mil glass-covered tungsten wire attached to a small magnetic slug. The wire was ground flush with the glass. The slug could traverse a 20 cm distance in a side arm through one of the small ports in the vacuum chamber. Thus, the normal to the face of the probe was perpendicular to the magnet field vector. The probe could be moved radially without otherwise disturbing the plasma.

Two probe circuits were used. The circuit used to measure the electron temperature is shown in Fig. 6.1a. Keithly electrometers were used for the ammeter and the voltmeter. The probe voltage was scanned by changing the resistance from probe to ground across a 10-turn potentiameter. The electron temperature was determined from the slope of a plot of log i_e vs v_p. The ion saturation current was subtracted from the total probe current to obtain i_e. The ion density was then determined from the ion saturation

Fig. 6.1a. Probe circuit for measuring T_e.

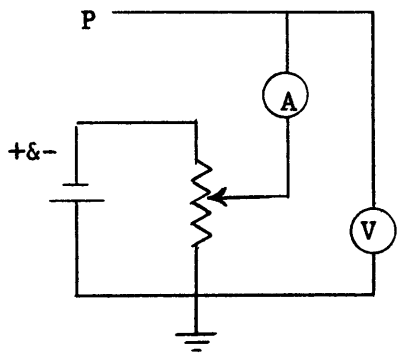

Fig. 6.1b. Probe circuit for measuring n_+ using the 60 Hz line source.

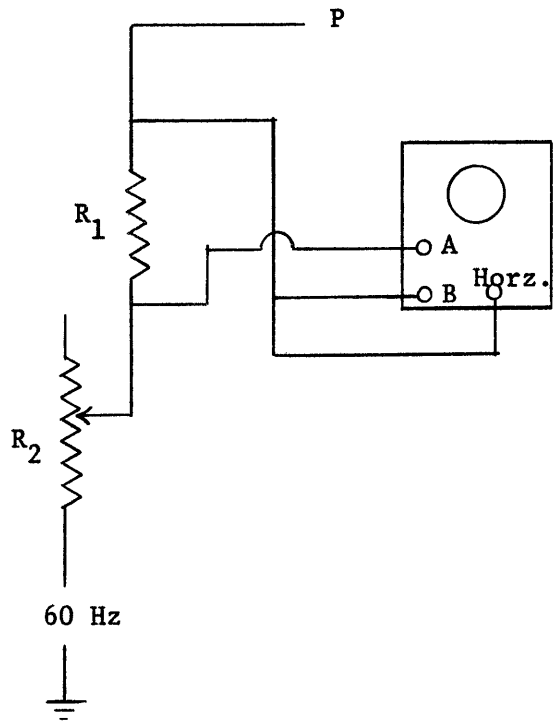

current. A probe curve obtained using this circuit is shown in Fig. 6.2.

To obtain rapid measurements of the density, the probe voltage was automatically scanned at 60 Hz by connecting the probe to the laboratory 60 Hz line source. This circuit is shown in Fig. 6.1b. The voltage across R_1 is proportional to the current drawn by the probe. This voltage was applied to the vertical deflection plates of an oscilloscope. The voltage of the probe with respect to ground was applied to the horizontal deflection plates. A scope picture of a typical probe curve is redrawn in Fig. 6.3.

3. Result of Probe Measurements

The value of the electron temperature obtained by averaging four probe determinations, taken at a distance of 1.5 cm from the center of the discharge under typical conditions, was

$$T_e = 15{,}100 \pm 4870\ ^{o}K \simeq 1.3\ eV. \qquad (6.7)$$

The electron density was calculated from the ion saturation current obtained from the scope pictures such as the one shown in Fig. 6.3, using Eq. 6.6 with $T_e = 1.3$ eV. The density is shown in Fig. 6.4 as a function of the radial distance from the center of the discharge.

B. Electron Temperature Determined from Helium Line Ratios

The electron temperature in the discharge was determined from the intensity ratio of the He II line at 4686 Å to the He I line at 5876 Å. Mewe [1967] has calculated this ratio for a steady helium plasma which is optically thin toward these lines. These calculations were made for electron temperatures between 2 and 11 eV and densities between 10^{16} and 10^{25} m^{-3}. This ratio is plotted in Fig. 6.5 as a function of T_e for three values of

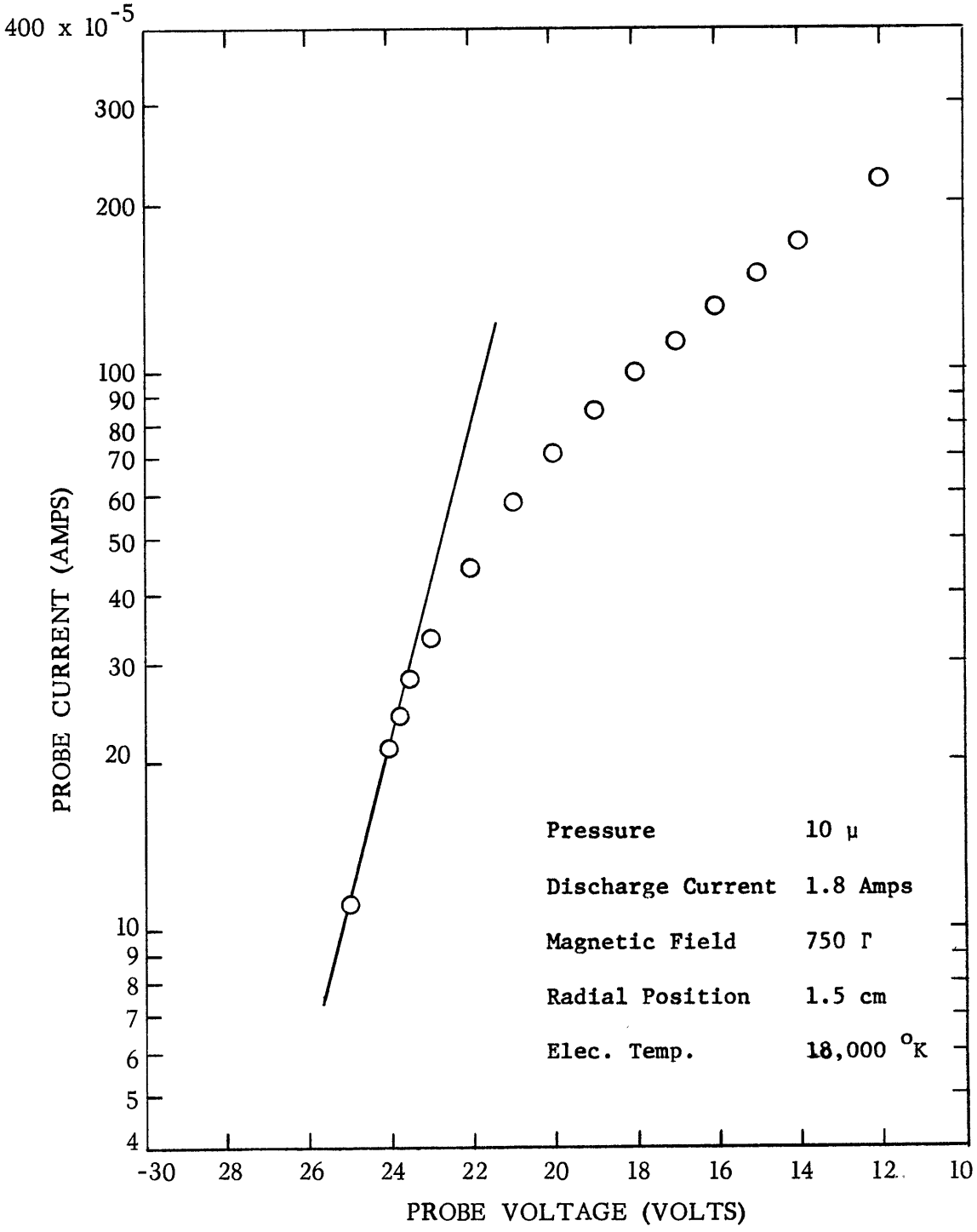

Fig. 6.2. A typical probe curve taken with the circuit shown in Fig. 6.1a. The difference between the total current to the probe and the ion saturation current is shown as a function of the probe voltage with respect to the anode.

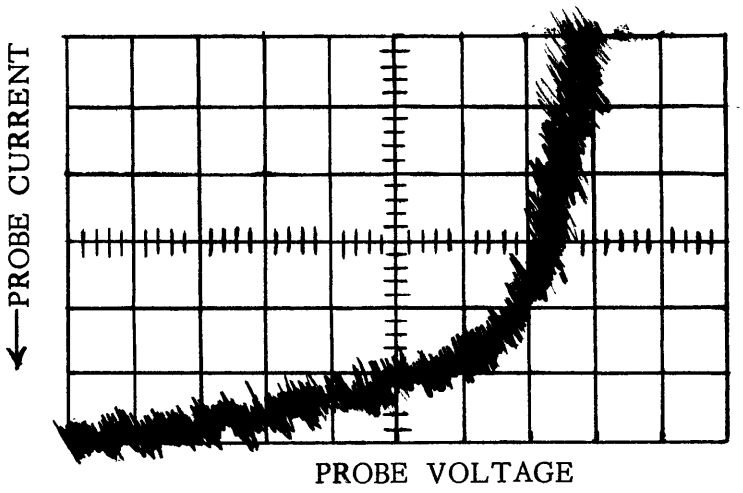

Fig. 6.3. A typical probe curve taken with the circuit shown in Fig. 6.1b. Drawing was made from a picture of the scope trace. Pressure = 10 μ, Discharge current = 2.0 Amps, Magnetic field = 1000 Γ, Radial position = 1.5 cm.

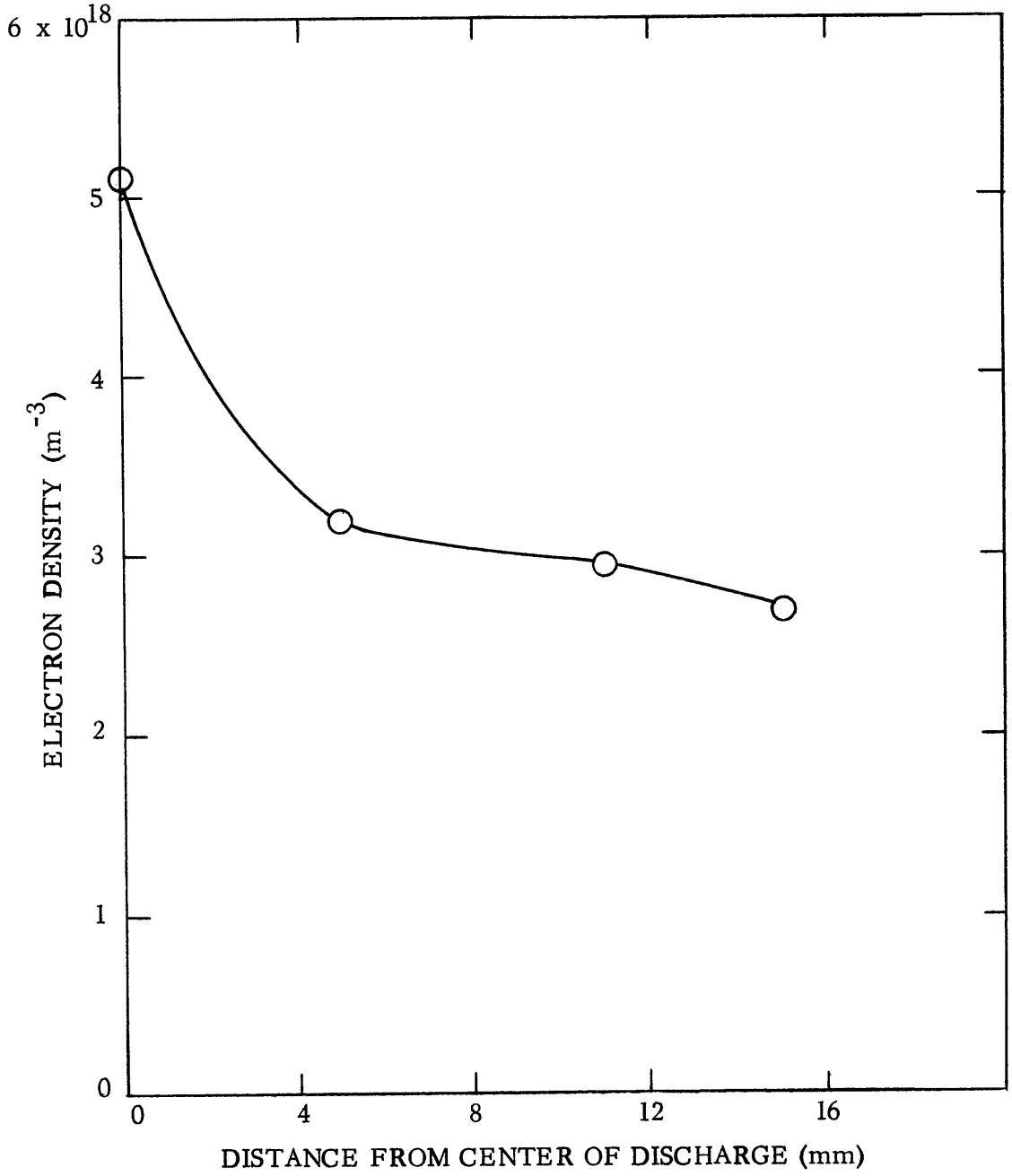

Fig. 6.4. The electron density as a function of the radius for T_e = 1.3 eV

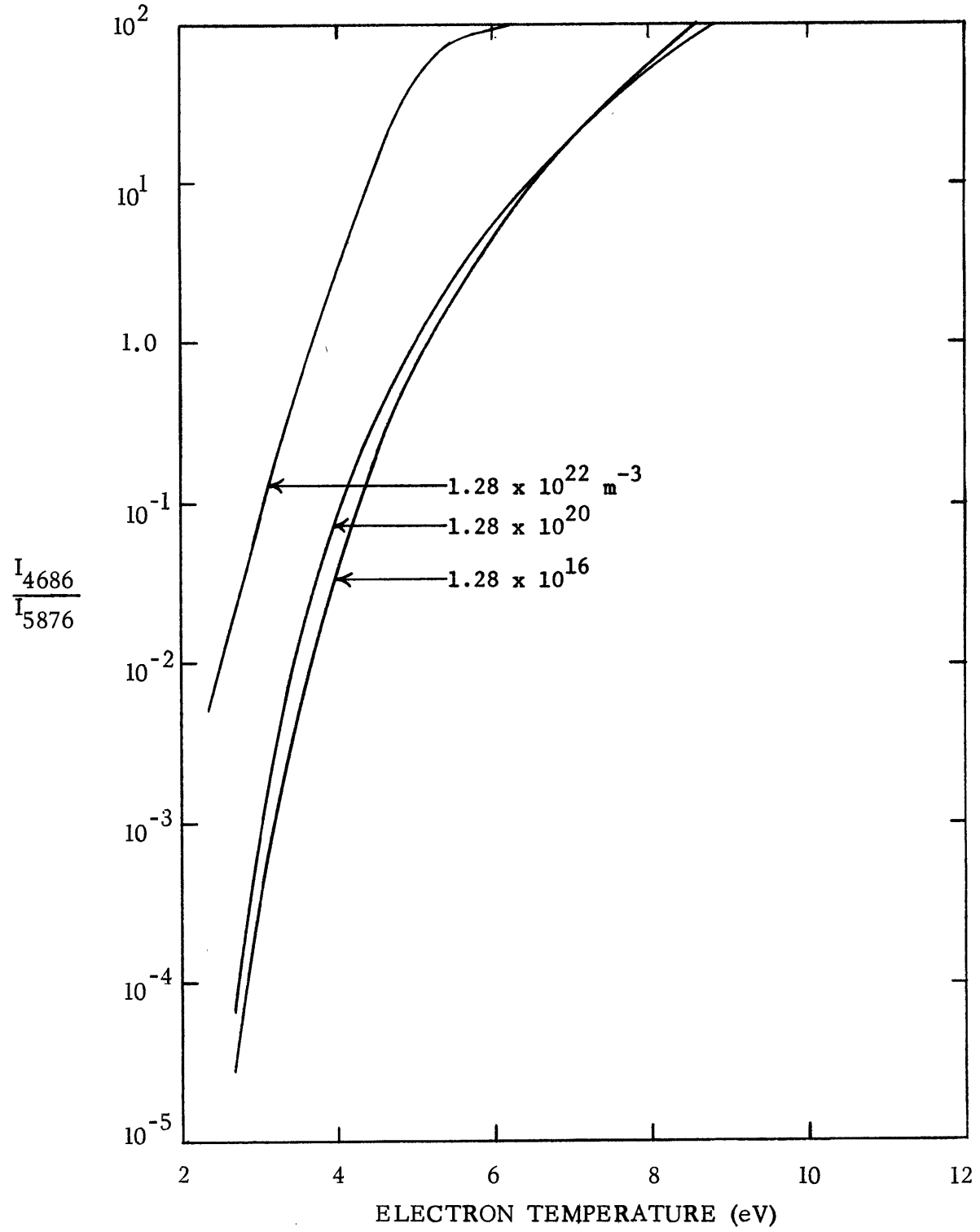

Fig. 6.5. The ratio of the intensities of the He II line at 4686 Å to the He I line at 5876 Å as a function of the electron temperature for $d' = d\left(\frac{kT_e}{kT_i}\right)^{1/2} = 10$ cm. Plotted from Table 4 in Mewe [1967].

the electron density. This ratio is nearly independent of the density for the values of the density used in this experiment.

The plasma was scanned through a plexiglass window in a side port with a Jarrell-Ash Model 82-020 Scanning Spectrometer. A slit limited the field of view to a 4 mm width across the plasma. A mirror was used to select the radial position observed. A diagram of the apparatus is shown in Fig. 6.6. An RCA 7265 photomultiplier detected the light output from the exit slit of the spectrometer. Photons detected by the photomultiplier were counted by a TSI Model 385-R Counter for periods of ten seconds. The dark current was subtracted from each count.

The ratio I_{4686}/I_{5876} at the center of the discharge was 1.9×10^{-4}, corresponding to an electron temperature of

$$T_e = 2.8 \text{ eV} = 32{,}500\ ^{o}\text{K}, \tag{6.8}$$

from Fig. 6.5. This value is significantly larger than the value measured by either the probe or the cw laser scattering. This discrepancy will be discussed in Chapter VIII.

The radial dependence of the intensity of the two helium lines and of the continuum near 4880 Å is shown in Fig. 6.7. I_{4686}/I_{5876} is seen to be nearly independent of radius, indicating that the temperature is also nearly independent of radius.

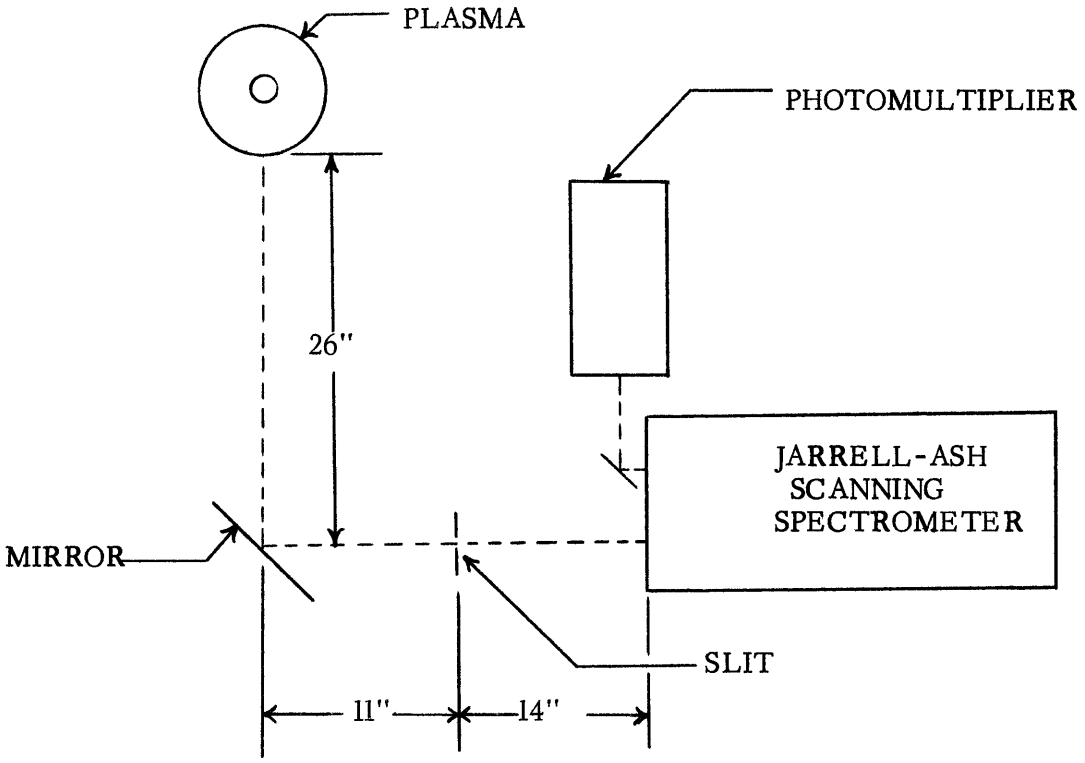

Fig. 6.6. Diagram of the apparatus for scanning spectral lines.

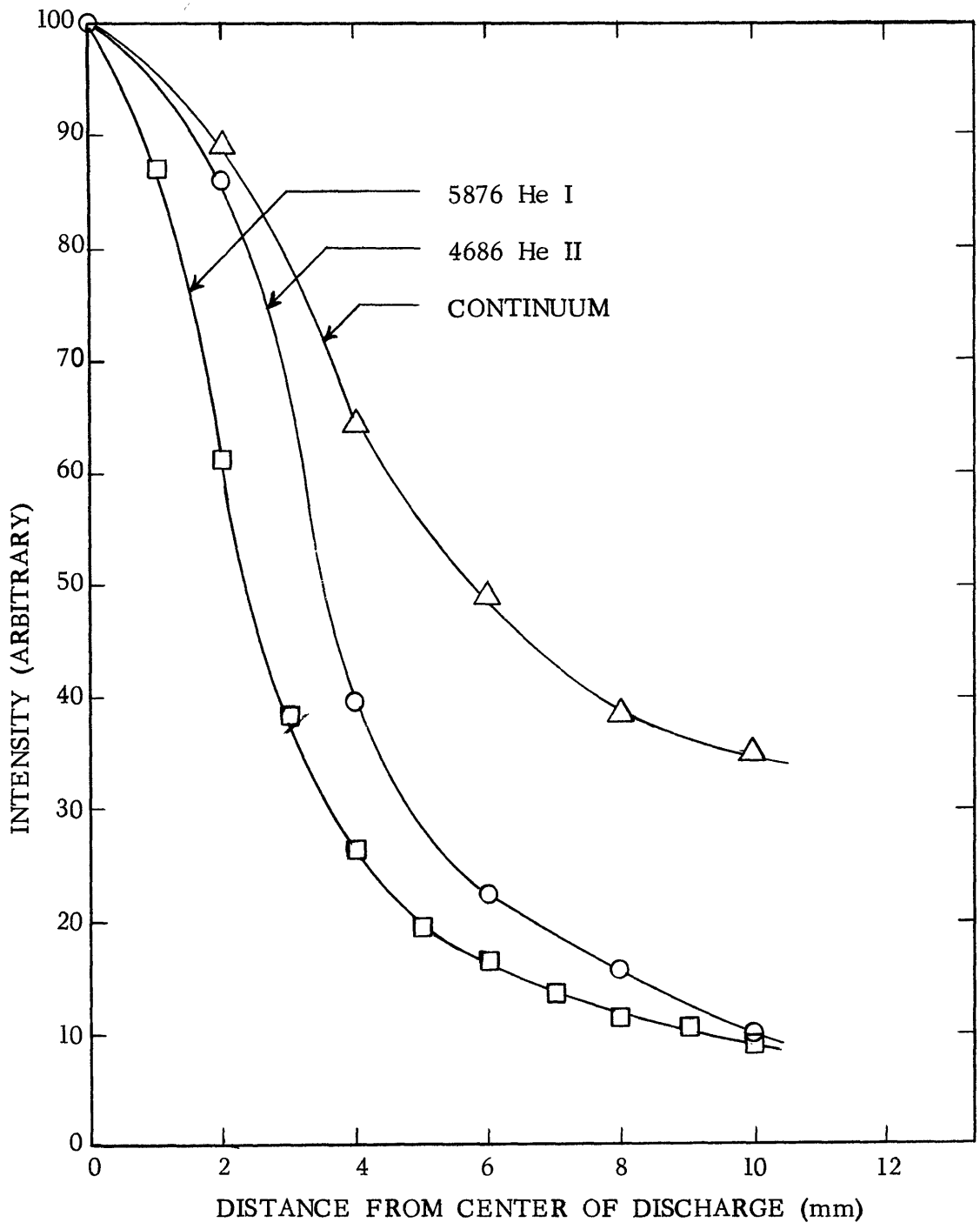

Fig. 6.7. The radial dependence of the intensity of continuum radiation near 4880 Å, the He II line at 4686 Å, and the He I line at 5876 Å. The intensity of each is normalized to 100 at the center.

CHAPTER VII

CONTINUOUS-WAVE LASER SCATTERING MEASUREMENTS

A. Experimental Procedure

The data was taken directly from the strip-chart recorder which traced the output of the lock-in amplifier as a function of time. A 100 second time constant was used on the lock-in amplifier. The zero level was first recorded on the chart before turning on the laser and the plasma. At a given angle of the rotatable interference filter, the signal obtained with only the plasma on was recorded for $7\frac{1}{2}$ minutes. This had a zero mean value since it consisted of noise with a time varying random phase with respect to the reference signal at 455 Hz. The laser was then unblocked for a 15 minute data run. The first $7\frac{1}{2}$ minutes of each such run were not analyzed. This time was taken to be sure that the detector had reached its dc output level. The data were read from the strip-chart every 15 seconds for the second $7\frac{1}{2}$ minutes of each run. These values were averaged and their standard deviation calculated.

The number of runs taken for both the $T_\perp$ measurements and the $T_\parallel$ measurements at a given rotation angle of the interference filter is shown in Table 7.1. Since the angle of the filter is taken with respect to an arbitrary zero, different values were used for the angles referring to each set of measurements. The mean value for the scattered intensity for each data run was normalized to a single laser power (0.5 Watts when measuring $T_\perp$ and 0.93 Watts when measuring $T_\parallel$). The mean values for a given rotation angle were then averaged to give the results presented in the next section.

Table 7.1 The number of data runs taken at a given rotation angle of the narrow-band interference filter.

$T_{\perp}$ Measurements

Rotation Angle	Data Runs
353^{o}	1
354	3
355	3
356	1
357	1
358	1

$T_{||}$ Measurements

Rotation Angle	Data Runs
0^{o}	1
1	1
2	2
3	2
4	3
5	2
6	2

B. Presentation of Data and Results

1. Electron Temperature

The output of the lock-in amplifier is shown in Figs. 7.1 and 7.2 as a function of the angle of the interference filter for the $T_\perp$ and the $T_\parallel$ measurements respectively. The spectrum is expected to be Gaussian if $\alpha << 1$, and the electrons have a thermal distribution. The value of α calculated for 8^o from the electron temperature (1.3 eV) and the electron density (3×10^{18} m^{-3}) obtained from the Langmuir probe data is 0.14.

The spectrum that is actually observed is the convolution of the instrumental spectral transmission with the spectrum of the scattered radiation. This convolution is given by the integral

$$S_{obs}(\lambda) = \int_{-\infty}^{+\infty} S_e(\Lambda) S_d(\lambda - \Lambda)\, d\Lambda, \qquad (7.1)$$

where S_{obs} is the observed spectrum, S_e is the spectrum of the scattered radiation, and S_d is the detector response. The detector response is assumed to have a Gaussian shape with a full width at half-height (FWHH), $\Delta\lambda_d = 1.58$ Å. The convolution integral has the property that the convolution of two Gaussian functions is also a Gaussian. If $\Delta\lambda_{obs}$ is the FWHH of the observed data, and $\Delta\lambda_e$ is the FWHH of the scattered radiation, this property implies that

$$\Delta\lambda_e^{\,2} = \Delta\lambda_{obs}^{\,2} - \Delta\lambda_d^{\,2} . \qquad (7.2)$$

If the observed spectrum is a Gaussian, a plot of the logarithm of the observed intensity as a function of $(\Delta\lambda/\lambda_o)^2$ will result in a straight line. This ratio can be obtained directly from the rotation angle of the interference filter. The ratio of the center wavelength of the passband of the filter to the center wavelength at perpendicular incidence is given by

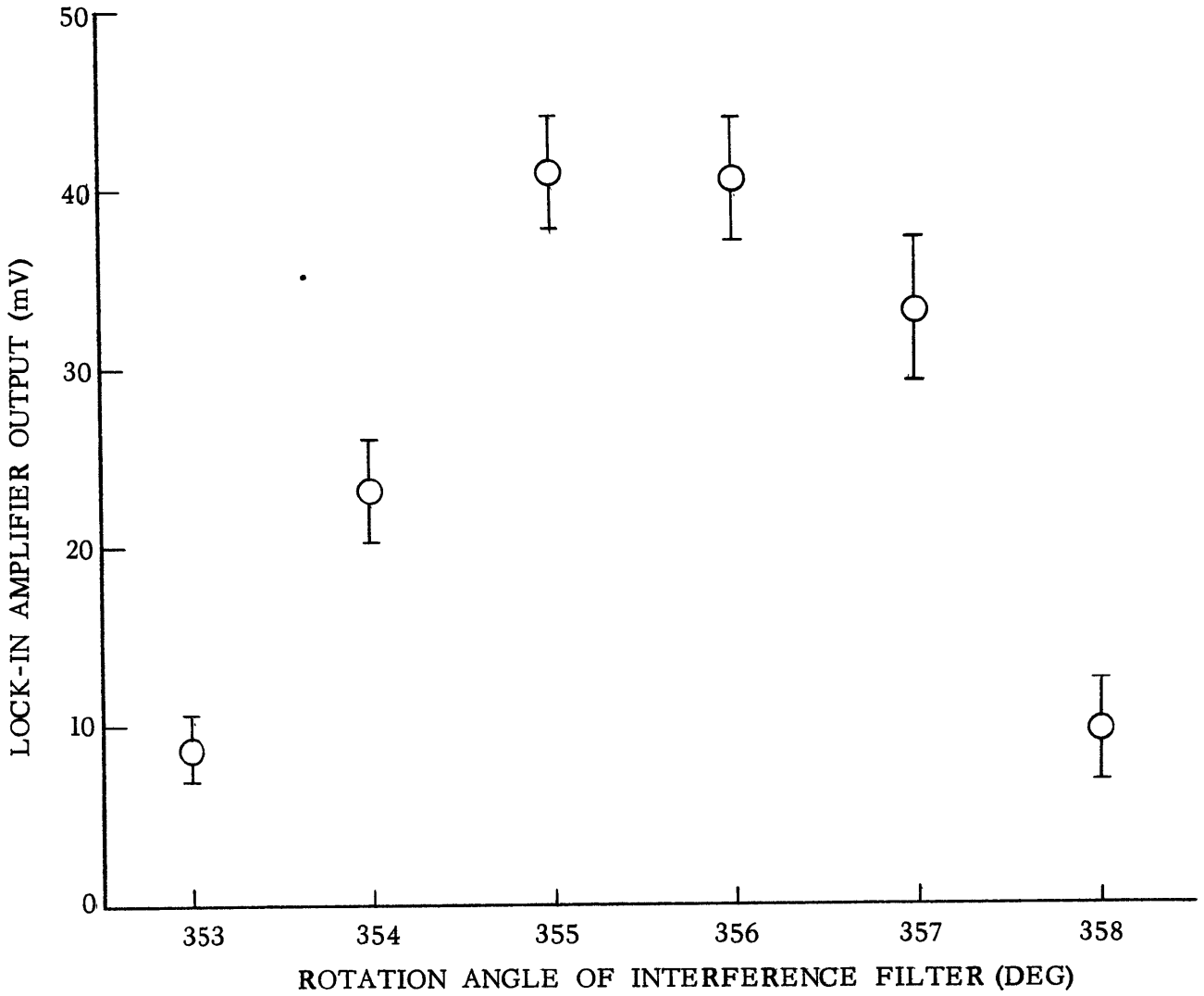

Fig. 7.1. Output of the lock-in amplifier as a function of the rotation angle of the rotatable filter for the $T_{\perp}$ measurements.

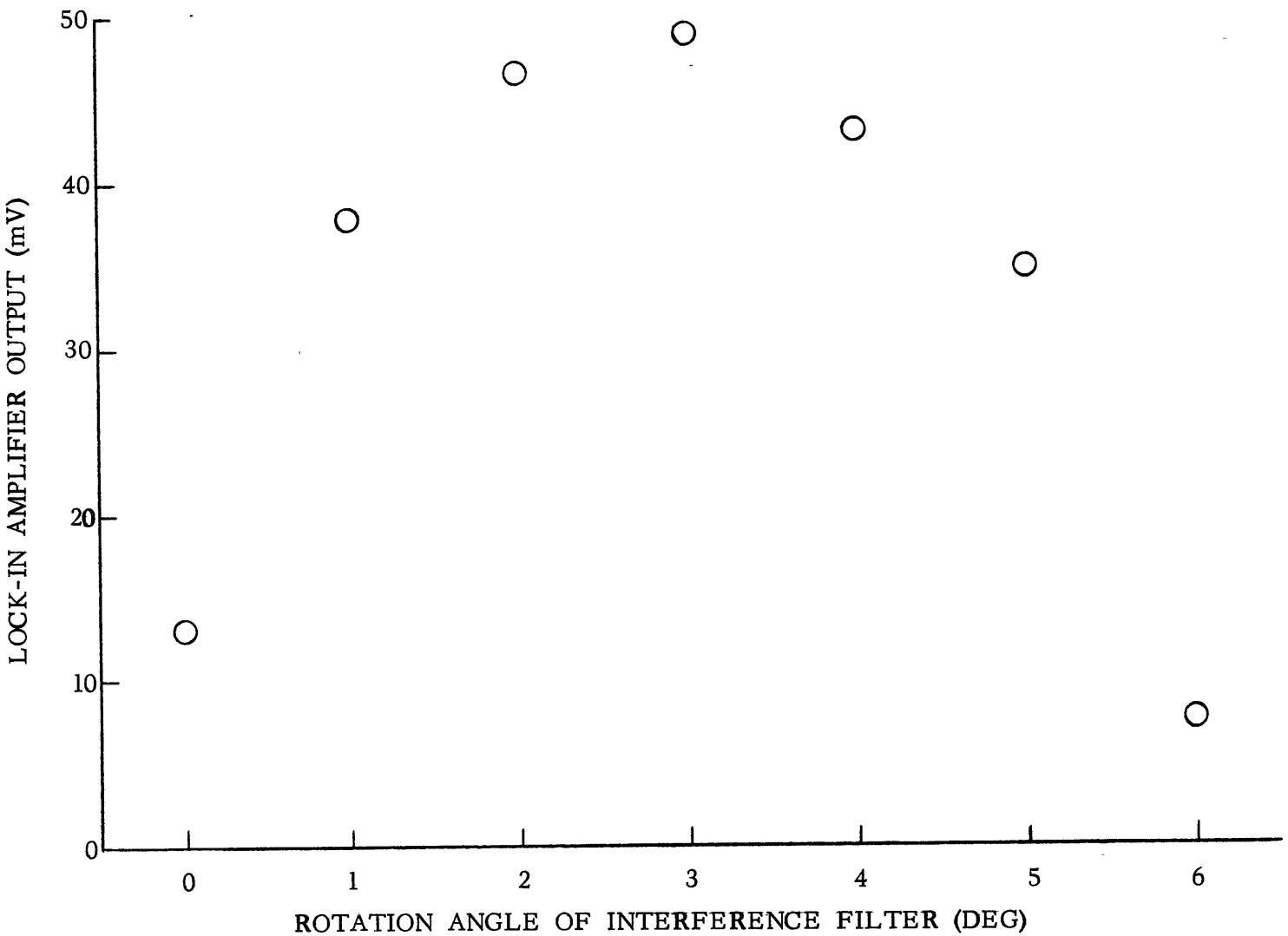

Fig. 7.2. Output of the lock-in amplifier as a function of the rotation angle of the rotatable filter for the $T_{||}$ measurements.

$$\frac{\Delta\lambda}{\lambda_\perp} = 1 - \left[\frac{(n^2 - \sin^2\Phi)^{1/2}}{n}\right] , \qquad (7.3)$$

where n is the index of refraction of the dielectric spacing material in the filter (taken to be 1.5), and Φ is the rotation angle of the filter away from normal incidence. The experimental data are replotted on a semilog graph in Fig. 7.3 using Eq. 7.3. $\Phi = 0$ was taken to be 355.5^o in Fig. 7.1, and 2.9^o in Fig. 7.2. The lines giving the best least-squares fit to the data are also drawn in Fig. 7.3. The values of $\Delta\lambda_{obs}^2$, obtained from the best-fit straight lines, are $6.64 \times 10^{-7}\ \lambda_\perp^2$ for the $T_\parallel$ measurement and $3.52 \times 10^{-7}\ \lambda_\perp^2$ for the $T_\perp$ measurement. The electron temperature both parallel and perpendicular to the magnetic field may be obtained from these values using Eq. 2.11. This equation may be written in terms of $\Delta\lambda_e$ as follows:

$$\frac{\Delta\lambda_e}{\lambda_o} = \frac{4 \sin\theta/2}{c} \{(2kT_e/m)\ \ln 2\}^{1/2}, \qquad (7.4)$$

where θ is the scattering angle, c is the velocity of light, k is Boltzmann's constant, and m is the mass of the electron. By assuming that $\lambda_o \simeq \lambda_\perp = 4880$ Å, the electron temperatures determined in this way from the laser scattering data are

$$T_\parallel = 30{,}800\ ^oK \qquad (7.5a)$$

$$T_\perp = 13{,}750\ ^oK. \qquad (7.5b)$$

The average electron temperature may be obtained from these values. This will be discussed in the next chapter.

2. Electron Density

With the detection scheme utilized in the experiments, the scattered

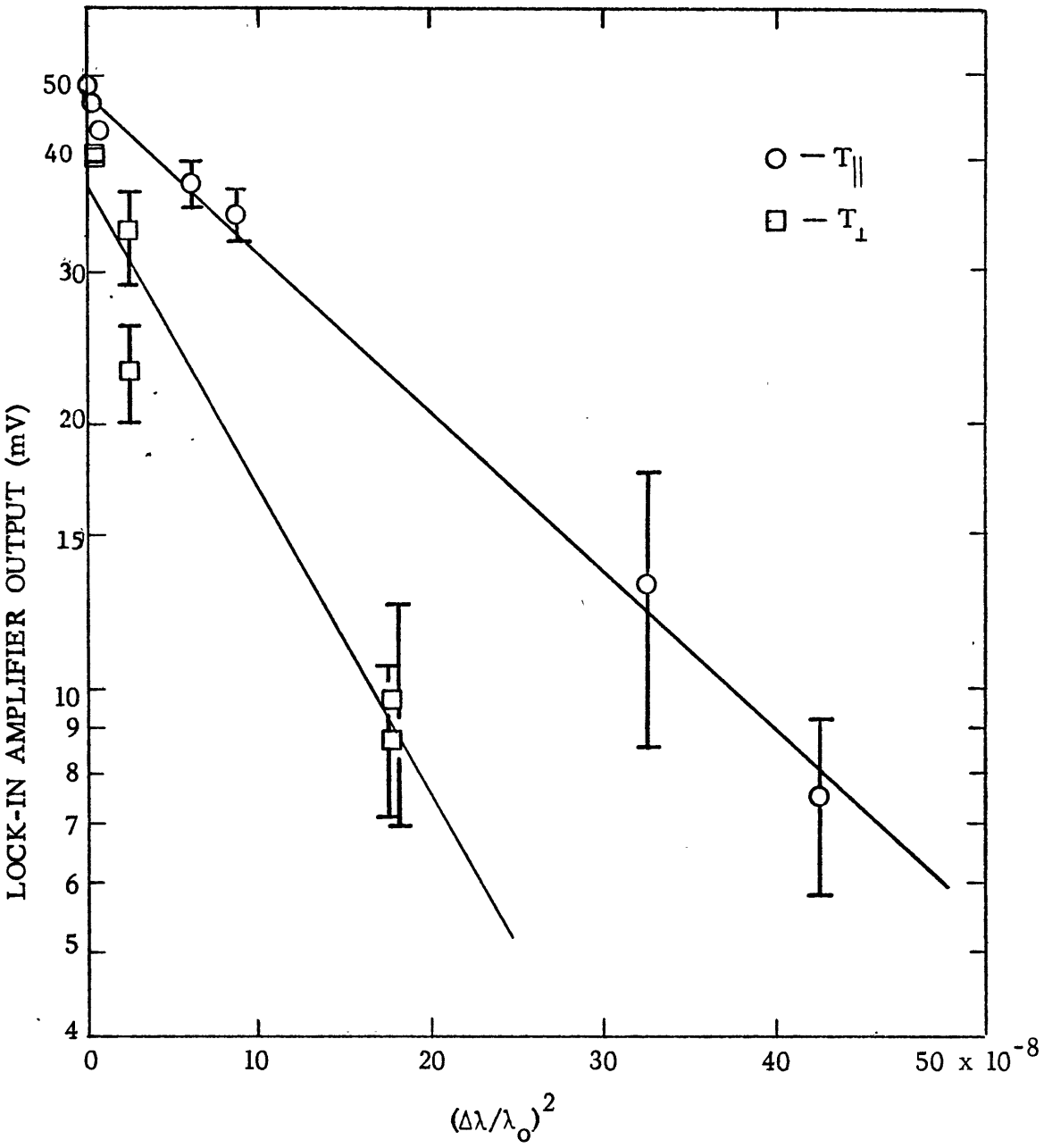

Fig. 7.3. Thomson scattering intensity vs $(\Delta\lambda/\lambda_o)^2$.

signal represents the effect of the imposed plasma modulation. We assume that the temperature of the electrons does not change and only the electron density is affected by the modulation. To demonstrate that this assumption is reasonable, the ion saturation current to a probe was measured as a function of the current through the discharge. The result is plotted in Fig. 7.4. Bohm et al. [1949] have shown that the ion saturation current is a function of the electron temperature and the ion density when a moderate magnetic field is present. The saturation current is given by

$$I_+ = 0.4\ n_+ eA(2kT_e/M_+)^{1/2}, \tag{7.6}$$

where e is the electron charge, A is the area of the probe, k is Boltzmann's constant, and M_+ is the mass of the ion. Since the ionization potential of helium is large, the predominant ion is the singly ionized helium ion. Thus, the ion density and the electron density are approximately equal. The fact that the ion saturation current varied linearly with the discharge current is a reasonable indication that the electron temperature is constant and that the electron density varies linearly with the current.

The value of the electron density modulation ΔN_e was also obtained from the scattering data. The power scattered from the incident laser beam per unit solid angle is given by Eq. 2.9. If N_{ph} is the total number of photons scattered per unit time into a solid angle Ω, we find from Eq. 2.9 that

$$N_{ph} h\nu = \frac{d\sigma}{d\Omega} I_o N_e L\Omega\ , \tag{7.7}$$

where h is Planck's constant, ν is the frequency of the scattered radiation, $\frac{d\sigma}{d\Omega} = 7.95 \times 10^{-30}\ m^2 sr^{-1}$ is the differential scattering cross section for

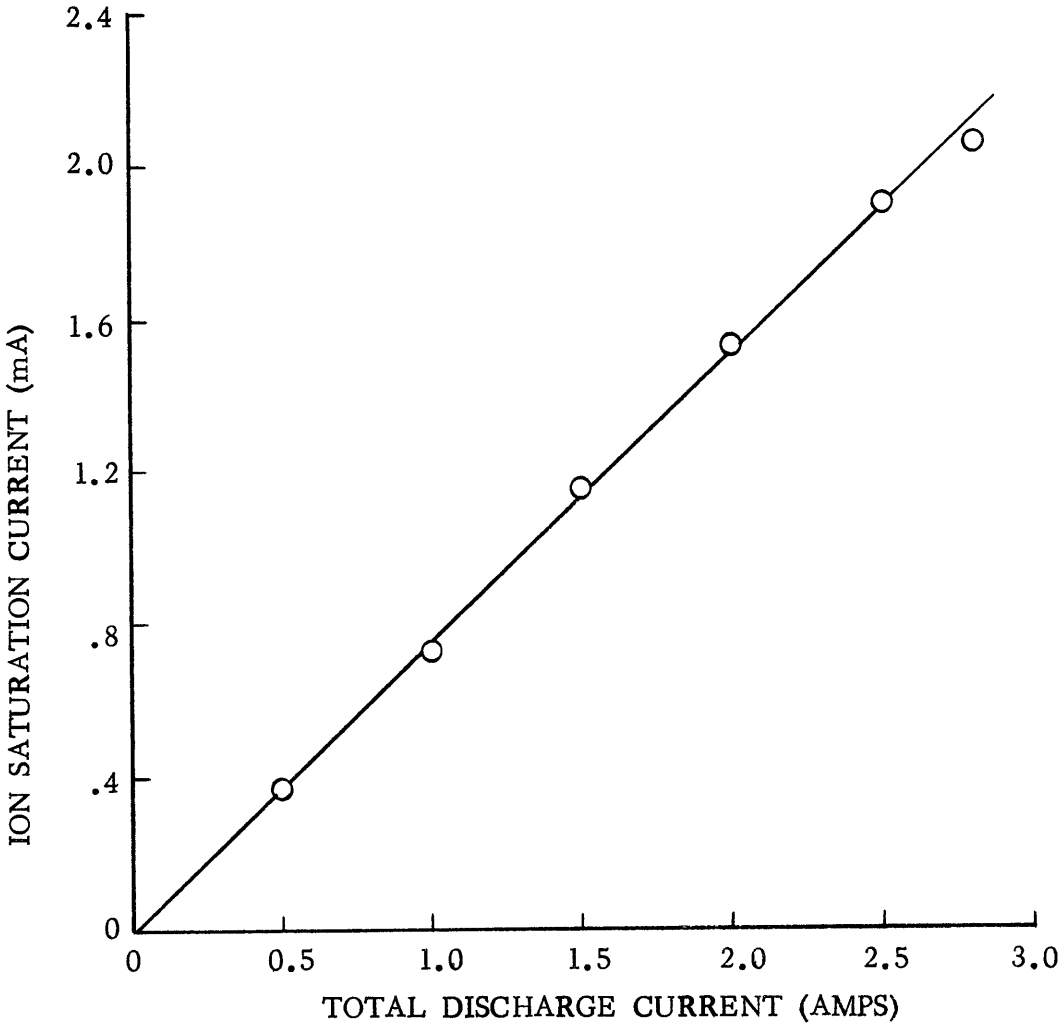

Fig. 7.4. Ion saturation current to a probe held at -40 Volts with respect to the anode vs the total current through the discharge.

Thomson scattering, I_o is the laser power, and L = 5 cm is the length of the scattering volume. If the peak-to-peak electron density modulation is ΔN_e, the density N_e may be expanded in the form

$$N_e = N_o + \frac{\Delta N_e}{2} [1 + \sin \omega_p t + \ldots], \tag{7.8}$$

where ω_p is the plasma modulation radian frequency. The laser power may be similarly expanded:

$$I_o = \frac{I_{max}}{2} [1 + \sin \omega_L t + \ldots]. \tag{7.9}$$

The product of these terms in Eq. 7.7 becomes

$$\begin{aligned} N_e I_o \simeq & \frac{N_o I_{max}}{2} [1 + \sin \omega_L t] \\ & + \frac{\Delta N_e I_{max}}{4} [1 + \sin \omega_p t + \sin \omega_L t + \sin \omega_p t \sin \omega_L t]. \end{aligned} \tag{7.10}$$

Using the identity $\sin A \sin B = \frac{1}{2} [\cos(A-B) - \cos(A+B)]$, this may be written

$$\begin{aligned} N_e I_o \simeq & \frac{N_o I_{max}}{2} [1 + \sin \omega_L t] \\ & + \frac{\Delta N_e I_{max}}{4} [1 + \sin \omega_p t + \sin \omega_L t] \\ & + \frac{\Delta N_e I_{max}}{8} \{\cos[(\omega_p - \omega_L)t] - \cos[(\omega_p + \omega_L)t]\} . \end{aligned} \tag{7.11}$$

The only component of $N_e I_o$ detected by the lock-in amplifier is the one at the sum frequency, $\omega_p + \omega_L$. Thus the scattered signal in phase with the reference signal is

$$\Delta N_{ph} = \frac{\Delta N_e I_{max}}{8} \frac{d\sigma}{d\Omega} \frac{\Omega \lambda_o L}{hc} \cos[(\omega_p + \omega_L)t + \pi]. \tag{7.12}$$

The number of photoelectrons emitted at the photocathode in phase with the reference signal is related to ΔN_{ph} by

$$\Delta N_{pe} = \eta \, \Delta N_{ph}, \tag{7.13}$$

where η is the efficiency of the optical system. ΔN_{pe} was determined by integrating the absolute scattered signal over the Gaussian spectrum which gave the best fit to the data. The gain of the photomultiplier and of the 1-Hz bandwidth amplifier were taken into account. The factor η may be separated into several terms:

$$\eta = \eta_{QE} \times \eta_{pf} \times \eta_{f1} \times \eta_{f2}, \tag{7.14}$$

where $\eta_{QE} = 0.18$ is the quantum efficiency of the photomultiplier at 4880 Å, and $\eta_{pf} = 0.8$, $\eta_{f1} = 0.8$, and $\eta_{f2} = 0.4$ are the transmission factors of the polaroid filter, the wide-band interference filter, and the narrow-band interference filter respectively. The values used for all of these parameters were either measured in the laboratory or provided as calibrations by the manufacturers.

The values obtained from Eqs. 7.12 and 7.13 for the peak-to-peak electron density modulation were

$$(\Delta N_e)_{\parallel} = 4.9 \times 10^{18} \ m^{-3}, \tag{7.15a}$$

from scattering parallel to the magnetic field and

$$(\Delta N_e)_{\perp} = 4.8 \times 10^{18} \ m^{-3}, \tag{7.15b}$$

from scattering perpendicular to the magnetic field.

Since the density varied approximately linearly with the current through the discharge, the electron density obtained from the probe data at a dc current of 1.8 Amps should agree with the peak-to-peak electron density modulation for a current modulation of 1.8 Amps. The value of ΔN_e obtained from the laser scattering data is in reasonable agreement with the probe measurements shown in Fig. 6.4.

The value of the scattering parameter α calculated from the values of the electron density and temperature obtained from the scattering measurements perpendicular to the magnetic field is 0.15. Since this is considerably less than one, the spectrum of the scattered radiation is expected to be approximately Gaussian and the method used to analyze the data is consistent with the results.

CHAPTER VIII

DISCUSSION OF RESULTS

A. Electron Temperature Asymmetry

The temperature obtained from the scattering data in one plane is the temperature T_j corresponding to the average energy $\langle E_j \rangle$ of one component of the electron velocity distribution. The relationship between T_j and $\langle E_j \rangle$ is

$$\langle E_j \rangle = \frac{1}{2} m \langle v_j^2 \rangle = \int_{-\infty}^{+\infty} \frac{1}{2} m v_j^2 \left(\frac{m}{2\pi k T_j}\right)^{1/2} \exp(-m v_j^2/2kT_j)\, dv_j$$

$$= \frac{1}{2} kT_j \, . \tag{8.1}$$

If we choose one axis of our coordinate system to be parallel to the magnetic field, for this axis

$$\langle E_{\parallel} \rangle = \frac{1}{2} kT_{\parallel} = eV_{\parallel} \, , \tag{8.2}$$

where $V_{\parallel}$ is the average energy in electron volts parallel to $\hat{B}$. The other two axes are perpendicular to the magnetic field. We assume by symmetry that the average energy component along each is equal, so that

$$\langle E_{\perp} \rangle = kT_{\perp} = eV_{\perp} \, , \tag{8.3}$$

where $V_{\perp}$ is the average energy in electron volts perpendicular to the magnetic field. Eqs. 8.2 and 8.3 were used to compute the average electron energies given in the following table:

Scattering Plane	Electron Temperature	Average Electron Energy	Electron Density
Parallel to $\hat{B}$	30,800 ^{o}K	1.3 eV	4.9×10^{18} m^{-3}
Perpendicular to $\hat{B}$	13,750	0.6+0.6=1.2	4.8×10^{18}

Table 8.1. Summary of the results obtained from cw scattering measurements.

The average electron energy obtained from the scattering measurements is

$$\sum_{j=1}^{3} \langle E_j \rangle = 2.5 \text{ eV}.$$

The spectrum observed for scattering in each plane was centered about the wavelength of the laser line. There was no indication of a dip or flattening at the center of the observed spectrum. These facts indicate that the Doppler shifts observed were due to random velocities in the sense that no pronounced drift velocities were present.

The large energy asymmetry implies that energy is added to the electrons in a direction parallel to the magnetic field. This occurs in two ways. First, an electron emitted by one of the filaments will be accelerated away from the cathode by the electric fields in its vicinity. Since the electric field in this region is directed primarily parallel to the direction of the magnetic field, the acceleration will be predominantly parallel to $\hat{B}$, thus adding energy along this axis. The component of the electric field perpendicular to $\hat{B}$ will accelerate an electron to a drift velocity given by

$$\vec{v}_d = \frac{\vec{E} \times \vec{B}}{B^2} \tag{8.4}$$

in a direction which is also perpendicular to $\hat{B}$. The energy gain in this direction is small compared with the energy gain along the field lines.

Since a static electric field is conservative, an electron entering the "high" electric field region between a cathode-anode pair will have its kinetic energy converted to potential energy until it is reflected and leaves this region. It will not gain kinetic energy. If, however, it makes a collision in this region and some of its parallel energy is converted to perpendicular energy, it will be accelerated by the electric field. As discussed above, this acceleration is primarily parallel to the magnetic field. Such a collision could be a two-particle Coulomb collision, an electron-neutral collision, or an encounter with the microscopic electric fields of stochastic fluctuations or coherent oscillations. With respect to the latter, microwave emission peaks have been observed near the electron cyclotron harmonics under similar conditions from the discharge used for these experiments [Breeding, 1965].

The mean free path for an electron-neutral collision for a 1.7 eV electron in helium at the pressure used in these experiments is 5 cm [Brown, 1959]. This is approximately the size of the "high-field" region at each end of the discharge. Therefore, an electron may gain parallel energy each time its axial oscillation brings it into this region. Collisions in the "low-field" region between the anodes would not be as effective a means of asymmetrizing the energy.

B. Comparison of the Temperatures Obtained from the Probe Data and the Scattering Data

The electron temperature measured by the Langmuir probe (15,100 ^{o}K) agrees reasonably well with the value obtained from the scattering data for the temperature perpendicular to the magnetic field (13,750 ^{o}K). However, it is considerably lower than the value obtained for the temperature parallel to the magnetic field (30,800 ^{o}K). This indicates that in the presence of a strong magnetic field, the electron retarding field of a probe, whose face is parallel to the magnetic field lines, acts only on the electron velocity component which is perpendicular to the magnetic field.

C. Absolute Determination of Electron Density

The experiments reported in this thesis have demonstrated that an accurate absolute measurement of the electron density can be obtained with a carefully calibrated detector system. Previous scattering measurements, performed using a pulsed ruby laser, have required a relative calibration to obtain the electron density. For this calibration, Rayleigh scattering from a pure gas in the scattering chamber was used. This technique, however, could not be used in the cw experiments since the neutral gas density could not be modulated to permit synchronous detection.

D. Tests for External Mixing in the Detector System

In order to be sure that the component frequencies were not mixed at the photocathode of the photomultiplier or in the external circuitry, the experiment was simulated by allowing radiation from both a small light bulb and the laser to simultaneously illuminate the EMI photomultiplier. The

current through the bulb was modulated at 70 Hz and the laser beam was chopped at 385 Hz. At radiation levels more than three times as large as those used in the actual scattering experiments, no mixing was observed.

The width of the scattered spectrum is one of the best indications that the scattered signal was not spurious. The FWHH of the spectrum observed in the $T_\perp$ experiment was 2.9 Å. This is slightly less than twice the FWHH of the rotatable interference filter. It is concluded that the width of the observed spectrum is due to a Doppler shift of the scattered radiation caused by the motions of the electrons.

E. Linearity of the Scattered Signal with Laser Power

The power scattered per unit solid angle per unit frequency interval is given by Eq. 2.9. It depends linearly on the incident laser power I_o. To test that this dependence held in the experiment, three data runs were made at a fixed angle of 355^o of the narrow-band filter, each at a different laser power. The results are plotted in Fig. 8.1. The error brackets shown in the figure are the standard deviation of the signal for each run. Thus, they represent statistical errors, and do not include other effects which may hamper comparisons between different data runs. Such effects include changes in the plasma parameters, as well as changes in the optical system and the external circuitry. Every effort was made to minimize such effects. Nevertheless, it is clear from the figure that the runs were not repeatable within the statistical error for each run. The three points do, however, fit the straight line, drawn through zero in the figure, well enough to conclude that the scattered intensity was linearly dependent on the laser power.

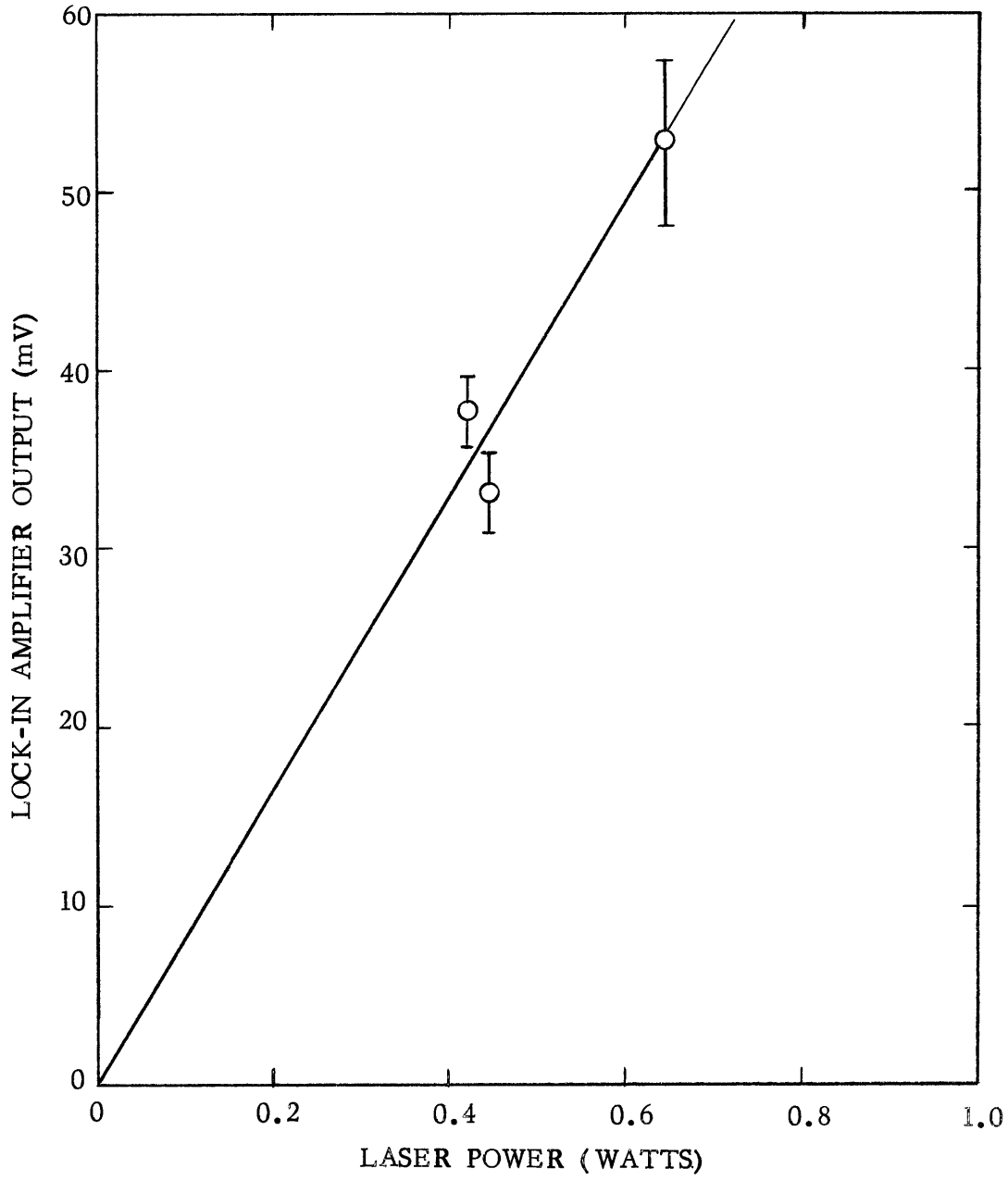

Fig. 8.1. Lock-in amplifier output vs laser power. Data taken at a fixed angle of the narrow-band interference filter.

F. Deviation of the Scattered Spectrum from a Gaussian

Referring to Fig. 7.3, it can be seen that one point at $(\Delta\lambda/\lambda_\perp)^2=2.3\text{x}10^{-8}$ deviates from the best-fit line considerably more than any of the other points. The question arises whether the departure of this one point is merely statistical and the electrons are thermalized, or if the departure is real, indicating a nonequilibrium condition in the distribution perpendicular to the magnetic field. Two arguments are available to indicate that it is statistical. First, the fact that this point departed from the Gaussian could imply that there was a bulk motion of the electrons in the plasma. If this were the case, the data point taken at the corresponding wavelength shift on the other side of λ_o would be expected to depart from the Gaussian in the opposite direction. Such was not the case. The corresponding point fell quite close to the best-fit line. Second, the wavelength shift corresponding to the data point in question was due to electrons whose energy was about 0.3 eV. An absence of large numbers of electrons of this particular energy in a helium plasma is difficult to understand because helium has no low energy excitation levels. Thus the deviation of this data point from the Gaussian is probably spurious.

G. Discussion of the Helium Line Ratio Electron Temperature Determination

The observed intensity ratio of the He II line to the He I line, I_{4686}/I_{5876}, when interpreted using Mewe's [1967] data, resulted in an electron temperature of 2.8 eV. This is considerably higher than the values obtained from the scattering data and from the probe data. The fundamental assumptions on which Mewe's calculations depend are: 1) The plasma is uniform, 2) it does not contain impurities which could contribute to the

electron density, 3) the plasma is fully contained, and 4) the particle densities must be greater than $10^{14} - 10^{15}\ d^{-1}\ cm^{-3}$, where d is the size of the plasma in centimeters. In the reflex discharge used for this experiment, all of these assumptions are invalid.

Optically, the plasma appeared to consist of several concentric cylinders. The innermost cylinder was roughly the diameter of the filaments. The second cylinder extended from the edge of the filaments to the inner radius of the anode annuli. A weak diffuse radiation came from the region outside of the anode annuli. Each cylinder represented a fairly sharp optical discontinuity; hence the plasma was definitely not uniform.

Many impurity lines were observed when scanning the entire spectrum with the spectrometer. Although no attempt was made to identify any of them, except those in the vicinity of 4880 Å, it is obvious that impurities with a much lower ionization potential than helium were present.

A reflex discharge is not a self-contained plasma. The hot filaments give off electrons which may attain fairly high energies in the potential well between the filaments. These travel along the magnetic field lines and sustain the plasma. They form a distribution which is distinct from the thermal electrons. Since the thermal electrons predominate, the high energy electrons were not observed in the scattering experiment. They would, however, excite the He II line resulting in a higher intensity ratio.

Finally, the plasma was about 10 cm in diameter. If this is taken to be d, then $10^{14}\ d^{-1} = 10^{13}\ cm^{-3} = 10^{19}\ m^{-3}$. This is greater than the electron density determined from the probe and scattering data by a factor of two.

In light of these circumstances, it is not surprising that the electron temperature obtained from the helium line ratios is inconsistent with that obtained from the probe and the scattering data.

CHAPTER IX

CONCLUSIONS AND SUGGESTIONS FOR FURTHER RESEARCH

A. Summary of Major Results

The experiments described in this thesis have demonstrated that Thomson scattering from a relatively low-power continuous-wave optical laser beam can be effectively used as a plasma diagnostic tool. The results obtained are in agreement with the theory for the regime $\alpha << 1$, as reviewed in Chapter II. The electron density measured by this technique agreed well with that obtained by Langmuir probe measurements.

An asymmetry was observed in the electron temperature. The temperature parallel to the imposed magnetic field was 30,800 ^{o}K, and the temperature perpendicular to the field was 13,750 ^{o}K. This asymmetry was qualitatively explained in terms of the energy sources and the velocity randomizing processes in the discharge. The temperature measured by a Langmuir probe agreed reasonably well with the electron temperature obtained by scattering from fluctuations perpendicular to the magnetic field. However, it was considerably lower that the temperature obtained by scattering from fluctuations parallel to the magnetic field.

It is concluded that a probe curve obtained from a plane probe whose face is parallel to a relatively large magnetic field, and analyzed according to the theory presented in Chapter VI, can only be used to obtain the electron temperature perpendicular to $\hat{B}$. The scattering technique is, however, a powerful tool for ascertaining the components of the particle velocity distributions.

B. Suggestions for Further Research

A scattering experiment with a spatial resolution better than the 5 cm resolution available in these experiments should be carried out, so that the electron temperature asymmetry could be determined as a function of radius. An attempt should be made to determine the exact cause of the asymmetry. The neutral gas pressure could be varied to determine the effect of collisions. If the asymmetry is found to depend entirely on collisions, the Boltzmann collision integral might be determined from the ratio of $T_{\perp}$ to $T_{||}$. If the magnetic field strength is decreased, the asymmetry would be expected to decrease. The electron energy perpendicular to $\hat{B}$ could be altered by illuminating the plasma with microwave radiation at the electron cyclotron frequency with its electric field perpendicular to $\hat{B}$.

Langmuir probe theory for plasmas in a magnetic field should be re-examined in light of the the electron asymmetry observed in the scattering measurements. This asymmetry may also effect diffusion, wave coupling, and radiation processes.

The experimental setup described in Chapter V may be used to measure or monitor the electron temperature and density in continuous plasma devices. A multichannel detector which could simultaneously observe the scattered intensity at several points in the spectrum would greatly facilitate its use as a diagnostic tool.

Continuous-wave laser scattering should now be extended to the region $\alpha > 1$. This will permit continuous measurements of the ion temperature, and will give an independent measure of the electron density from the wavelength shift of the electron satellite peaks with respect to the incident wavelength.

Values of $\alpha > 1$ are more easily realized using lasers which operate in the infrared. CO_2 lasers are now available with an output power of several hundred Watts at 10.6 μ. Such a laser could be used with a Hg-doped germanium detector and a synchronous detection system similar to the one used in this experiment.

The power available from a cw laser may be increased at least a factor of ten if the experiment is conducted within the laser cavity.

The reliability of the cw lasers, combined with the fact that scattering by a low-power source does not disturb the plasma, will make them a powerful diagnostic tool in the future.

BIBLIOGRAPHY

Akhiezer, A.I., I.G. Prokhoda, and A.G. Sitenko, Scattering of electromagnetic waves in a plasma, Soviet Phys. JETP, 6(33), 576-582, 1958.

Anastassiades, A.J., and T.C. Marshall, Scattering of microwaves from plasma spacecharge waves near the harmonics of the electron gyrofrequency, Phys. Rev. Letters, 18(25), 1117-1119, 1967.

Anderson, Oscar A., Measurement of the electron correlation spectrum in a plasma, Phys. Rev. Letters, 16(22), 978-980, 1966.

Arunasalam, V., and S.C. Brown, Experiment on microwave scattering from acoustic ion-plasma wave instability (abstract), Bull. Am. Phys. Soc., 9(4), 494, 1964.

Ascoli-Bartoli, U., J. Katzenstein, and L. Lovisetto, Scattering of a laser beam in a laboratory plasma (abstract), Bull. Am. Phys. Soc., 9(4), 495, 1964a.

Ascoli-Bartoli, U., J. Katzenstein, and L. Lovisetto, Forward scattering of light from a laboratory plasma, Nature, 204(4959), 672-673, 1964b.

Ascoli-Bartoli, U., J. Katzenstein, and L. Lovisetto, Spectrum of laser light scattered from a single giant pulse in a laboratory plasma, Nature, 207(4992), 63-64, 1965.

Baym, Gordon, and R.W. Hellwarth, Nonlinear interactions of radiation in plasmas, in Physics of Quantum Electronics, edited by P.L. Kelley, B. Lax, and P.E. Tannenwald, pp. 105-110, McGraw-Hill Book Co., N.Y., 1966.

Beach, A.D., A 12 channel, doppler profile spectrophotometer for plasma scattered laser light, UK Atomic Energy Authority AWRE Rep., April, 1967.

Berk, H.L., Incoherent electromagnetic scattering from driven plasma oscillations, Phys. Fluids, 7(6), 917-918, 1962.

Bernstein, Ira B., Waves in a plasma in a magnetic field, Phys. Rev., 109(1), 10-21, 1958.

Bohm, D., E.H.S. Burhop, and H.S.W. Massey, Use of probes for plasma exploration, in The Characteristics of Electrical Discharges in Magnetic Fields, edited by A. Guthrie and R.K. Wakerling, McGraw-Hill, N.Y., 1949.

Bottoms, P.J., and M. Eisner, Thermalization of cold electron-hot ion plasmas (abstract), Bull. Am. Phys. Soc., 12(5), 743, 1967.

Bowles, K.L., Observation of vertical-incidence scatter from the ionosphere at 41 Mc/sec, Phys. Rev. Letters, 1(12), 454-455, 1958.

Boyd, T.J.M., D.E. Evans, and J. Katzenstein, Light scattering by plasmas, Phys. Letters, 22(5), 589-591, 1966.

Brown, L.S., and T.W. Kibble, Interaction of intense laser beams with electrons, Phys. Rev., 133(3A), A705-A719, 1964.

Brown, T.S., and D.J. Rose, Determination of electron velocities by Thomson scattering (abstract), Bull. Am. Phys. Soc., 10(2), 226, 1965.

Brown, T.S., and D.J. Rose, Plasma diagnostics using lasers: relations between scattered spectrum and electron-velocity distribution, J. Appl. Phys., 37(7), 2709-2714, 1966.

Buneman, O.,Scattering of radiation by the fluctuations in a nonequilibrium plasma, J. Geophys. Res., 67(5), 2050-2053, 1962.

Chan, P.W., and R.A. Nodwell, Collective scattering of laser light by a plasma, Phys. Rev. Letters, 16(4), 122-124, 1966.

Cheng, H. and Y.C. Lee, Quantum theory of photon interaction in a plasma, Phys. Rev., 142(1), 104-114, 1966.

Consoli, T., C. Gormezano, et L. Slama, Diffusion de la lumiere d'un laser a rubis par un plasma dense, Phys. Letters, 20(3), 267-268, 1966.

Crosignani, B., and P. DiPorto, Statistical properties of coherent light scattered by a plasma, Phys. Letters, 24A(1), 69-70, 1967.

Daehler, Mark, and F.L. Ribe, Cooperative light scattering from theta-pinch plasmas (abstract), Phys. Rev. Letters, 19(1), A4, 1967a.

Daehler, M., and F.L. Ribe, Cooperative scattering from theta-pinch plasmas, Phys. Letters, 24A(13), 745-746, 1967b.

Daehler, M., and F.L. Ribe, A high-resolution, coherent, light-scattering experiment (abstract), Bull. Am. Phys. Soc., 12(5), 743, 1967c.

Daehler, Mark, and F.L. Ribe, Cooperative light scattering from θ-pinch plasmas, Phys. Rev., 161(1), 117-125, 1967d.

Davies, W.E.R., and S.A. Ramsden, Scattering of light from electrons in a plasma, Phys. Letters, 8(3), 179-180, 1964.

DeSilva, A.W., D.E. Evans, and M.J. Forrest, Observation of Thomson and co-operative scattering of ruby laser light by a plasma, Nature, 203(4952), 1321-1322, 1964.

DeSilva, A.W., D.E. Evans, and M.J. Forrest, Observation of Thomson and cooperative scattering of ruby-laser light by a plasma (abstract), Bull. Am. Phys. Soc., 10(2), 227, 1965.

Dougherty, J.P., and D.T. Farley, A theory of incoherent scattering of radio waves by a plasma, Proc. Roy. Soc. (London), A259, 79-99, 1960.

Dougherty, J.P., and D.T. Farley, Jr., A theory of incoherent scattering of radio waves by a plasma, J. Geophys. Res., 68(19), 5473-5486, 1963.

DuBois, D.F., and V. Gilinsky, Incoherent scattering of radiation by plasmas. I. Quantum mechanical calculation of scattering cross sections, Phys. Rev., 133(5A), A1308-A1316, 1964a.

DuBois, D.F., and V. Gilinsky, Incoherent scattering of radiation by plasmas. II. Effect of Coulomb collisions on classical plasmas, Phys. Rev., 133(5A), A1317-A1322, 1964b.

Evans, D.E., M.J. Forrest, and J. Katzenstein, Co-operative scattering of laser light by a thetatron plasma, Nature, 211(5044), 23-24, 1966a.

Evans, D.E., M.J. Forrest, and J. Katzenstein, Asymmetric co-operative scattered light spectrum in a thetatron plasma, Nature, 212(5057), 21-23, 1966b.

Evans, D.E., M.J. Forrest, and J. Katzenstein, Scattering of laser light by a thetatron plasma: I. The cooperative electron spectrum (abstract), Bull. Am. Phys. Soc., 12(5), 743, 1967a.

Evans, D.E., M.J. Forrest, and J. Katzenstein, Scattering of laser light by a thetatron plasma: II. The ion spectrum (abstract), Bull. Am. Phys. Soc., 12(5), 743-744, 1967b.

Farley, D.T., J.P. Dougherty, and D.W. Barron, A theory of incoherent scattering of radio waves by a plasma II. Scattering in a magnetic field, Proc. Roy. Soc. (London), A263, 238-258, 1961.

Farley, D.T., A theory of incoherent scattering of radio waves by a plasma, 4. The effect of unequal ion and electron temperatures, J. Geophys. Res. 71(17), 4091-4098, 1966.

Farrow, L.A., and S.J. Buchsbaum, Thomson scattering of cw laser light from electrons in a plasma (abstract), Bull. Am. Phys. Soc., 10(2), 226, 1965.

Feix, M.R., and K.U. von Hagenow, Connection between correlations and fluctuations in a plasma, Report IPP/6/37, 1965.

Fejer, J.A., Scattering of radio waves by an ionized gas in thermal equilibrium, Can. J. Phys., 38(8), 1114-1133, 1960a,

Fejer, J.A., Radio-wave scattering by an ionized gas in thermal equilibrium, J. Geophys. Res., 65(9), 2635-2636, 1960b.

Fejer, J.A., Scattering of radio waves by an ionized gas in thermal equilibrium in the presence of a uniform magnetic field, Can. J. Phys., 39(5), 716-740, 1961.

Fiocco G., and E. Thompson, Thomson scattering of optical radiation from an electron beam, Phys. Rev. Letters, 10(3), 89-91, 1963a.

Fiocco, G., and E. Thompson, Techniques for observing Thomson scattering of optical radiation from electrons (abstract), Bull. Am. Phys. Soc., 8(4), 372, 1963b.

Fried, Z., A note on non-linear effects in electrodynamics, Nuovo Cimento, 22(6), 1303-1305, 1961.

Fried Z., and W.M. Frank, Generation of "beats" from a microscopic viewpoint, Nuovo Cimento, 27(1), 218-227, 1963.

Fried, Z., Photon scattering in the low frequency, high intensity limit, Phys. Letters, 3(7), 349-351, 1963.

Fünfer, E., B. Kronast, and H.J. Kunze, Experimental results on light scattering by a θ-pinch plasma using a ruby laser, Phys. Letters, 5(2), 125-127, 1963a.

Fünfer, E., W.H. Kegel, B. Kronast, and H.J. Kunze, Local determination of plasma parameters in a θ-pinch plasma by light scattering experiments, in Comptes Rendus de la VI^{e} Conference International sur les Phenomenes D'Ionisation dans les Gaz, edited by P. Hubert and E. Cremieu-Alcan, pp. 119-121, Paris, 1963b.

George, T.V., L. Goldstein, L. Slama, and M. Yokoyama, Molecular scattering of ruby laser light, Phys. Rev., 137(2A), A369-A380, 1965.

Gerry, E.T., and R.M. Patrick, Thomson scattering computations for laboratory plasmas, Phys. Fluids, 8(1), 208-210, 1965.

Gerry, E.T., Plasma diagnostics by Thomson scattering of a laser beam, Ph.D. Thesis, Department of Nuclear Engineering, M.I.T., May, 1965a.

Gerry, E.T., Thomson scattering from a hollow-cathode arc plasma (abstract), Bull. Am. Phys. Soc., 10(2), 226, 1965b.

Gerry, Edward T., and D. Rose, Plasma diagnostics by Thomson scattering of a laser beam, J. Appl. Phys., 37(7), 2715-2724, 1966.

Gordon, W.E., Incoherent scattering of radio waves by free electrons with applications to space exploration by radar, Proc. IRE, 46(11), 1824-1829, 1958.

Granatstein, V.L., and S.J. Buchsbaum, Depolarization of microwaves scattered from fluctuations in a critically dense plasma (abstract), Bull. Am. Phys. Soc., 12(5), 742, 1967.

Hagfors, T., Density fluctuations in a plasma in a magnetic field, with applications to the ionosphere, J. Geophys. Res., 66(6), 1699-1712, 1961.

Hughes, T.P., A new method for the determination of plasma electron temperature and density from Thomson scattering of an optical maser beam, Nature, 194(4825), 268-269, 1962.

Ichimaru, Setsuo, Theory of fluctuations in a plasma, Annals of Phys., 20(1), 78-118, 1962a.

Ichimaru, S., D. Pines, and N. Rostoker, Observation of critical fluctuations associated with plasma-wave instabilities, Phys. Rev. Letters, 8(6), 231-233, 1962b.

Ivanov, A.A., and D.D. Ryutov, Scattering of electromagnetic waves by plasma oscillations in a plane plasma layer, Soviet Phys. JETP, 21(5), 913-916, 1965.

Izawa, Y., M. Yokoyama, and C. Yamanaka, Thomson scattering of ruby-laser light by a shock wave plasma, J. Phys. Soc. Japan, 21(8), 1610, 1966.

Jackson, J.D., Classical Electrodynamics, pp. 488-491, John Wiley & Sons, New York, 1962.

John, P.K., R. Benesch, and S.A. Ramsden, Measurement of the ion and electron temperatures in a θ-pinch plasma from the forward scattering of a ruby laser beam (abstract), Bull. Am. Phys. Soc., 12(5), 743, 1967.

Johnson, W.B., Laser interferometry and photon scattering in plasma diagnostics, IEEE Trans. Antennas Propagation, AP-15(1), 152-162, 1967.

Kegel, W.H., The laser as a tool for plasma diagnostics, Report IPP/6/9, 1963.

Kegel, W.H., Lichtstreuung und Mischung in einem Plasma, Report IPP/6/21, 1964, (In German).

Kegel, W.H., Light mixing and the generation of the second harmonic in a plasma in an external magnetic field, Zeitschrift für Naturforschung, 20a, 793-800, 1965.

Kroll, N.M., A. Ron, and N. Rostoker, Optical mixing as a plasma density probe, Phys. Rev. Letters, 13(3), 83-86, 1964.

Kroll, N.M., Nonlinear optical effects in plasmas, in Physics of Quantum Electronics, edited by P.L. Kelley, B. Lax, and P.E. Tannenwald, pp. 86-104, McGraw-Hill Book Co., N.Y., 1966.

Kronast, B., Laser application in the field of plasma physics (abstract), Z. Angew. Math. Phys. (Switzerland), 16(1), 120, 1965, (Laser-Physics and Applications Symposium, Bern, 1964.).

Kronast, B., H. Röhr, E. Glock, H. Zwicker, and E. Fünfer, Measurements of the ion and electron temperature in a theta-pinch plasma by forward scattering, Phys. Rev. Letters, 16(24), 1082-1085, 1966.

Kunze, H.J., E. Fünfer, B. Kronast, and W.H. Kegel, Measurement of the spectral distribution of light scattered by a θ-pinch plasma, Phys. Letters, 11(1), 42-43, 1964a.

Kunze, H.J., A. Eberhagen, and E. Fünfer, Electron density and temperature measurements in a 26 kJ θ-pinch by light scattering, Phys. Letters, 13(1), 38-39, 1964b.

Kunze, H.J., E. Fünfer, and H. Röhr, Electron temperature measurements in a megajoule theta-pinch by light scattering, Phys. Letters, 19(1), 11-12, 1965a.

Kunze, H.J., Messung der lokalen Elektronentemperatur und Elektronendichte in einem Θ-Pinch mittels der Streuung eines Laserstrahls, Zeitschrift für Naturforschung, 20a, 801-813, 1965b, (In German).

Laaspere, T., On the effect of a magnetic field on the spectrum of incoherent scattering, J. Geophys. Res., 65(12), 3955-3959, 1960.

Lambe, G.L., The scattering of electromagnetic waves by nonequilibrium plasmas, Los Alamos Scientific Lab. Report LA-2715, 1962.

Lidsky, L.M., D.J. Rose, and E. Thompson, Model for anomalous radiation in Thomson-scattering experiments, Quarterly Progress Report No. 69., Research Laboratory of Electronics, M.I.T., pp. 98-105, 1964.

Malyshev, G.M., Plasma diagnostics by light scattering on electrons, Soviet Phys. Tech. Phys., 10(12), 1633-1643, 1966.

Malyshev, G.M., G.V. Ostrovskaya, G.T. Razdobarin, and L.V. Sokolova, Measurement of electron temperature and concentration in an arc plasma via Thomson scattering of laser light, Soviet Phys. Doklady, 11(5), 441-442, 1966.

Mandel, L., Thomson scattering of intense light beams, J. Opt. Soc. Am., 54(2), 265, 1964.

Mewe, R., Relative intensity of helium spectral lines as a function of electron temperature and density, Brit. J. Appl. Phys., 18, 107-118,1967.

Mizushima, M., Scattering of very intense electromagnetic waves, Phys. Rev., 132(2), 951-954, 1963.

Moorcroft, D.R., On the power scattered from density fluctuations in a plasma, J. Geophys. Res., 68(16), 4870-4872, 1963

Nguyen-Quang-Dong, On the scattering of light by a plasma, Phys. Letters, 21(2), 159-160, 1966.

Pappert, R.A., Incoherent scatter from a hot plasma, Phys. Fluids, 6(10), 1452-1457, 1963.

Patrick, R.M., and E.T. Gerry, Thomson-scattering observations from MHD shock-heated plasmas (abstract), Bull. Am. Phys. Soc., 10(2), 226, 1965.

Patrick, Richard M., Thomson scattering measurements of magnetic annular shock tube plasmas, Phys. Fluids, 8(11), 1985-1994, 1965.

Penney, C.M., An optical diagnostic technique for high density plasmas, Nuclear News, 6(7), 21, 1963.

Perkins, F.W., E.E. Salpeter, and K.O. Yngvesson, Incoherent scatter from plasma oscillations in the ionosphere, Phys. Rev. Letters, 14(15), 579-581, 1965.

Piliya, A.D., The scattering of waves in a plasma in the presence of a mode conversion, Soviet Phys. Tech. Phys., 11(12), 1967.

Pineo, V.C., L.G. Kraft, and H.W. Briscoe, Ionospheric backscatter observation at 440 Mc/s, J. Geophys. Res., 65(5), 1620-1621, 1960a.

Pineo, V.C., L.G. Kraft, and H.W. Briscoe, Some characteristics of ionospheric backscatter observed at 440 Mc/s, J. Geophys. Res., 65(9), 2629-2633, 1960b.

Pineo, V.C., and H.W. Briscoe, Discussion of incoherent backscatter power measurements at 440 Mc/s, J. Geophys. Res., 66(11), 3965-3966, 1961.

Pineo, V.C., and D.P. Hynek, Spectral widths and shapes and other characteristics of incoherent backscatter from the ionosphere observed at 440 megacycles per second during a 24-hour period in May, 1961, J. Geophys. Res., 67(13), 5119-5129, 1962.

Platzman, P.M., and N. Tzoar, Light-off-light scattering in a plasma medium (abstract), Bull. Am. Phys. Soc., Ser. II, 9(4), 495, 1964a.

Platzman, P.M., S.J. Buchabaum, and N. Tzoar, Light-off-light scattering in a plasma, Phys. Rev. Letters, 12(21), 573-575, 1964b.

Ramsden, S.A., and W.E.R. Davies, Radiation scattered from the plasma produced by a focused ruby laser beam, Phys. Rev. Letters, 13(7), 227-229, 1964.

Ramsden, S.A., and W.E.R. Davies, Scattering of a laser beam from a θ-pinch plasma (abstract), Bull. Am. Phys. Soc., 10(2), 227, 1965.

Ramsden, S.A., R. Benesch, W.E.R. Davies, and P.K. John, Observation of cooperative effects and determination of the electron and ion temperatures in a plasma from the scattering of a ruby laser beam, IEEE J. Quantum Electronics, QE-2(8), 267-270, 1966.

Ramsden, S.A., and W.E.R. Davies, Observation of cooperative effects in the scattering of a laser beam from a plasma, Phys. Rev. Letters, 16(8), 303-306, 1966.

Ramsden, S.A., P.K. John, B. Kronast, and R. Benesch, Evidence for a thermonuclear reaction in a θ-pinch plasma from the scattering of a ruby laser beam, Phys. Rev. Letters, 19(12), 688-689, 1967.

Renau, Jacques, Scattering of electromagnetic waves from a nondegenerate ionized gas, J. Geophys. Res., 65(11), 3631-3640, 1960.

Renau, J., H. Camnitz, and W. Flood, The spectrum and the total intensity of electromagnetic waves scattered from an ionized gas in thermal equilibrium in the presence of a static quasi-uniform magnetic field, J. Geophys. Res., 66(9), 2703-2732, 1961.

Renau, J., The cross section for scattering of electromagnetic waves from an ionized gas in thermal nonequilibrium, J. Geophys. Res., 67(9), 3624-3626, 1962.

Renau, J., Notes on number density fluctuations and the scattering cross section for electromagnetic waves scattered from a thermal nonequilibrium plasma, Zeitschrift für Physik, 177, 458-494, 1964.

Röhr, H., A 90° laser scattering experiment for measuring temperature and density of the ions and electrons in a cold dense theta pinch plasma, Phys. Letters, 25A(2), 167-168, 1967.

Ron, A., J. Dawson, and C. Oberman, Influence of collisions on scattering of electromagnetic waves by plasma fluctuations, Phys. Rev., 132(2), 497-498, 1963.

Rosen, P., Scattering of electromagnetic waves by longitudinal plasma waves, Phys. Fluids, 3(3), 416-417, 1959.

Rosenbluth, M.N., and N. Rostoker, Scattering of electromagnetic waves by a nonequilibrium plasma, Phys. Fluids, 5(7), 776-788, 1962.

Rostas, F., Les methodes de diagnostic des plasmas utilisant des lasers, J. Phys. (France), 27(5-6), 367-384, 1966. (In French)

Salat, A., and A. Schlüter, Plasma diagnostics by nonlinear resonant angle scattering, Phys. Letters, 14(2), 106-107, 1965.

Salat, A., Microscopic description of a plasma and nonlinear incoherent light scattering, Report IPP/6/49, 1966. (In German)

Salpeter, E.E., Electron density fluctuations in a plasma, Phys. Rev., 120(5), 1528-1535, 1960a.

Salpeter, E.E., Scattering of radio waves by electrons above the ionosphere, J. Geophys. Res., 65(6), 1851-1852, 1960b.

Salpeter, E.E., Effect of the magnetic field in ionosphere backscatter, J. Geophys. Res., 66(3), 982-984, 1961a.

Salpeter, E.E., Plasma density fluctuations in a magnetic field, Phys. Rev., 122(6), 1663-1674, 1961b.

Salpeter, E.E., Density fluctuations in a nonequilibrium plasma, J. Geophys. Res., 68(5), 1321-1333, 1963.

Schwarz, S.E., Scattering of optical pulses from a nonequilibrium plasma, Proc. IEEE, 51(10), 1362, 1963.

Schwarz, S.E., Plasma diagnostics by means of optical scattering, J. Appl. Phys., 36(6), 1836-1841, 1965.

Sigman, D.R., J.F. Holt, and M.L. Pool, Thomson scattering of laser light from a plasma (abstract), Bull. Am. Phys. Soc., 10(2), 226, 1965.

Stehle, P., High-intensity limit of Thomson scattering, J. Opt. Soc. Am., 53(8), 1003, 1963.

Stern, R. A., Microwave reflection from small-diameter plasma columns, J. Appl. Phys., 34(9), 2562-2565, 1963.

Stern, R. A., Interaction of resonant plasma oscillations in a low-pressure Hg discharge, Appl. Phys. Letters, 4(4), 80-82, 1964.

Stern, R.A., and N. Tzoar, Incoherent microwave scattering from resonant plasma oscillations, Phys. Rev. Letters, 15(11), 485-488, 1965.

Stern, R.A., Harmonic generation and frequency mixing at plasma resonance, Phys. Rev. Letters, 14(14), 538-540, 1965.

Taylor, E.C., and G.G. Comisar, Frequency spectrum of thermal fluctuations in plasmas, Phys. Rev., 132(6), 2379-2384, 1963.

Theimer, O., High density corrections to the scattering cross section of a plasma, Phys. Letters, 20(6), 639-640, 1966.

Thompson, E., and G. Fiocco, Measurements of large-angle scattering of laser radiation from d.c. plasmas, in Comptes Rendus de la VI^{e} Conference International sur les Phenemenes D'Ionisation dans les Gaz, edited by P. Hubert and E. Cremieu-Alcan, pp. 111-112, Paris, 1963a.

Thompson, E., and G. Fiocco, Thomson scattering of optical radiation from a thermal plasma (abstract), Bull. Am. Phys. Soc., 8(4), 372, 1963b.

Thompson, W.B., Dynamic interferometry as a plasma probe (abstract), Bull. Am. Phys. Soc., 12(5), 743, 1967.

Vachaspati, Scattering of light by free electrons: intensity dependent phase shift and frequency change, Indian J. Pure Appl. Phys., 2(12), 373-376, 1964.

Van Zandt, T.E., and K.L. Bowles, Use of the incoherent scatter technique to obtain ionospheric temperatures, J. Geophys. Res., 65(9), 2627-2628, 1960.

Verweij, W., Probe measurements and determination of electron mobility in the positive column of low-pressure mercury-argon discharges, Ph.D. Thesis, University of Utrecht, 1960.

Villars, F., and V.F. Weisskopf, On the scattering of radio waves by turbulent fluctuations of the atmosphere, Proc. IRE, 43(10), 1232-1239, 1955.

Wada, J.Y., Scattering of microwaves from a traveling-wave density modulated plasma column of finite length (abstract), Bull. Am. Phys. Soc., 12(5), 742, 1967.

Weichel, H., P.V. Avizonis, and D.F. Vonderhaar, Observation of plasma ion oscillations in a laser-produced plasma, Phys. Rev. Letters, 19(1), 10-12, 1967.

Weinstock, J., Correlation functions, and scattering of electromagnetic waves by inhomogeneous and nonstationary plasmas (abstract), Bull. Am. Phys. Soc., 12(5), 742, 1967.

Wharton, C.B., and J.H. Malmberg, Microwave scattering from plasma waves (abstract), Bull. Am. Phys. Soc., 12(5), 742, 1967.

Williamson, J.H., R.A. Nodwell, and A.J. Barnard, Computed profiles for electromagnetic radiation scattered from a plasma, J. Quant. Spectrosc. Radiat. Transfer., 6(6), 895-898, 1966.

Additions:

Breeding, R.J., Investigations of a reflex discharge, Master's Thesis, M.I.T., 1965.

Brown, S.C., Basic Data of Plasma Physics, The Technology Press of M.I.T., Cambridge, Mass., 1959, p. 5.

BIOGRAPHICAL NOTE

The author was born on March 29, 1942, in McKeesport, Pennsylvania. He graduated from McKeesport High School in 1959. At the Massachusetts Institute of Technology, he majored in physics, and received a Bachelor of Science Degree in 1963. Since Fall 1963, he has been a graduate student in the Department of Geology and Geophysics at M. I. T. He held a National Science Foundation Traineeship from September 1966 to September 1967. The summers of 1963 and 1965 were spent with the Atomic and Molecular Science R&D Group at the Westinghouse Research and Development Center in Pittsburgh, Pennsylvania.

Publications include:

Fiocco, G., H.C. Koons, and M.L. Meeks, Search for comet Ikeya-Seki (1965f) at 8 Gc/sec and 15 Gc/sec, Quarterly Progress Report No. 80, Research Laboratory of Electronics, M.I.T., Jan. 1966.

Schulz, G.J., and H.C. Koons, Energy levels of the compound state of N_2 near 2.3 eV, J. Chem. Phys., 44(3), 1297-1298, 1966.

Koons, H.C., and Giorgio Fiocco, Measurements of the density and temperature of electrons in a reflex discharge by scattering of continuous-wave Ar^+ laser light, J. Appl. Phys. (To be published).